Energy density profiles in critical films

M. Krech,[1] E. Eisenriegler,[2] and S. Dietrich[1]

[1]*Fachbereich Physik, Bergische Universität Wuppertal, Postfach 100127, 42097 Wuppertal, Federal Republic of Germany*

[2]*Institut für Festkörperforschung, Forschungszentrum Jülich, Postfach 1913, 52425 Jülich, Federal Republic of Germany*

(Received 7 February 1995)

Scaling density profiles of critical O(N)-symmetric systems confined to a film geometry are analyzed by field-theoretic renormalization-group techniques in $d=4-\varepsilon$ spatial dimensions. At bulk criticality we explicitly calculate the energy density profile for five different boundary conditions and determine their corresponding universal scaling functions. In order to discuss the influence of the boundary conditions at the two surfaces of the film on the global shape of the profiles, a suitable exponentiation scheme is constructed. Using these exponentiated scaling functions as well as results from conformal field theory, the shapes of the energy density profiles in $d=2,3$, and 4 are compared. Finally, we discuss the short-distance behavior of the energy density profiles close to the surfaces of the film as it follows from the knowledge of the full profiles in first order ε.

PACS number(s): 64.60.Fr, 05.70.Jk, 68.15.+e, 68.35.Rh

I. INTRODUCTION

The thermodynamic behavior of systems in the vicinity of their critical or multicritical points can be described successfully by means of field-theoretic methods [1,2]. The field-theoretic renormalization group provides systematic approximations for universal quantities such as critical exponents or certain amplitude combinations [3,4] by, e.g., a perturbation expansion around the upper critical dimension d_c with $d_c=4$ in the case of a standard critical point. Within this framework thermodynamic quantities of critical systems are governed by *scaling operators* $\Psi(\mathbf{r})$ that are *local* quantities. In the language of the well-known Φ^4 theory (see Sec. II), the most common examples for such scaling operators are the *order parameter field* $\Phi(\mathbf{r})$ and the *energy density field* $-\frac{1}{2}\Phi^2(\mathbf{r})$. In spatially homogeneous and isotropic systems the thermal average $\langle\Psi(\mathbf{r})\rangle$ of a single scaling operator $\Psi(\mathbf{r})$ is a constant ψ_b. Surfaces break this spatial symmetry so that the thermal average of $\Psi(\mathbf{r})$ exhibits a spatial variation. For $\Psi(\mathbf{r})=\Phi(\mathbf{r})$ one obtains the order parameter profile $m(\mathbf{r})=\langle\Phi(\mathbf{r})\rangle$ and setting $\Psi(\mathbf{r})=-\frac{1}{2}\Phi^2(\mathbf{r})$ yields the energy density profile $e(\mathbf{r})=-\frac{1}{2}\langle\Phi^2(\mathbf{r})\rangle$. In a semi-infinite geometry, which is bounded by a plane wall such that the z component of the position vector $\mathbf{r}=(\mathbf{r}_\parallel,z)$ measures the distance from this wall, these profiles are particularly simple. The system is still homogeneous and isotropic with respect to $\mathbf{r}_\parallel$ and therefore any scaling density profile is only a function of z. At a critical point of the bulk system the z dependence of the scaling density profile $\langle\Psi(\mathbf{r})\rangle_{\infty/2}$ in a corresponding semi-infinite system is already fixed by the requirement that $\langle\Psi(\mathbf{r}_\parallel,z\to\infty)\rangle_{\infty/2}=\psi_b$ and by the *scaling dimension* x_Ψ of $\Psi(\mathbf{r})$. For distances z from the wall that are large compared to microscopic length scales one finds [5]

$$\langle\Psi(\mathbf{r}_\parallel,z)\rangle_{\infty/2}-\psi_b=A_\Psi z^{-x_\Psi}\ , \tag{1.1}$$

where A_Ψ is a nonuniversal amplitude. The scaling dimension x_Ψ in Eq. (1.1) is given by $x_\Psi=\beta/\nu$ for the magnetization density and by $x_\Psi=(1-\alpha)/\nu$ for the energy density, where α, β, and ν are the critical exponents of the specific heat, the order parameter, and the bulk correlation length, respectively. Note that Eq. (1.1) holds only for distances z that are large compared to microscopic length scales. In fact, the spatial variation of, say, the magnetization profile near the boundary of a semi-infinite Ising lattice is governed by the lattice constant, which ensures the existence of a *finite* value of the magnetization density at the surface. Likewise, in a binary liquid mixture the molecular diameter provides the microscopic scale on which the composition profile crosses over to a finite value at a wall immersed into the fluid. The presence of a microscopic length scale therefore serves as a cutoff for the scaling density profiles as given by Eq. (1.1) at microscopic distances from a wall where nonuniversal properties become important.

For thermodynamic conditions slightly off the critical point the power law in Eq. (1.1) is replaced by the scaling law (see, e.g., Ref. [6])

$$\langle\Psi(\mathbf{r}_\parallel,z)\rangle_{\infty/2}-\psi_b=A_\Psi z^{-x_\Psi}f_\pm(z/\xi_\pm)\ , \tag{1.2}$$

which again holds only for macroscopic distances z from the wall. Here $f_+(y_+)$ denotes a *universal scaling function* for $T>T_{c,b}$ and $f_-(y_-)$ denotes the corresponding scaling function for $T<T_{c,b}$ with the property $f_\pm(0)=1$, where $T_{c,b}$ denotes the bulk critical temperature. For short-ranged interactions and within the Ising universality class (see Sec. II) the macroscopic distance z from the wall in the argument $y_\pm=z/\xi_\pm$ is scaled by the *bulk correlation length* $\xi_\pm=\xi_0^\pm|(T-T_{c,b})/T_{c,b}|^{-\nu}$ above *and* below the bulk critical temperature $T_{c,b}$, respectively. Note that the property $f_\pm(0)=1$ of the scaling function ensures that in the limit $T\to T_{c,b}$, Eq. (1.2) reduces to Eq. (1.1) for $T\to T_{c,b}$.

From the literature one knows several examples of scaling density profiles in semi-infinite geometries in

$d=4-\varepsilon$ that have been calculated by field-theoretic renormalization-group methods. The energy density profile $e(z)$ has been discussed in Ref. [6] for $T \geq T_{c,b}$ and the ordinary surface universality class (see Sec. II and Ref. [5]). The order parameter profile $m(z)$ in a semi-infinite geometry is of special interest in the context of critical adsorption [7]. The full profile $m(z)$ above and below bulk criticality [see Eq. (1.2)] has recently been calculated for the extraordinary transition, i.e., in the presence of a surface field h_1 within the Ising universality class [8]. Furthermore, the energy density profile enters the exact variational formulation of two-dimensional layered Ising models [9].

In a film geometry a second wall is present at $z=L$, where L is the thickness of the film. Scaling density profiles in films can be studied under both *local* and *global* aspects. In the first case one is interested in the perturbation of the profile near one wall, i.e., at $z \ll L$, due to the presence of the other (far) wall at $z=L$. This perturbation has become known as the *distant wall correction* or the *critical wall perturbation* [10–12]. To give an example, let Φ represent the composition of a binary liquid mixture close to its critical demixing point ($T=T_c$, $\Phi=\Phi_c$) [10] (see also Ref. [13]). A plate that is immersed into the mixture will generally show a preferential affinity for one of the components. *At* the critical demixing point the local average composition $m_{\infty/2}(z)=\langle\Phi(\mathbf{r})\rangle-\Phi_c$ at a distance z from the wall will then deviate from zero according to Eq. (1.1) with the exponent $x_\Phi=\beta/\nu$. In the magnetic language of the Ising universality class the plate is characterized by a *surface field* h_1, which induces either $m(0)>0$ or $m(0)<0$, i.e., it prefers either one component or the other depending on the sign of h_1 [10]. The distant wall correction imposed on the composition profile $m_{\infty/2}(z)$ by the presence of a *second* plate immersed into the critical binary liquid mixture at a distance L from the first plate can be expressed by the corresponding film profile $m_{\text{film}}(z)$ at small distances z [12]

$$m_{\text{film}}(z \ll L)=m_{\infty/2}(z)\left[1+B\left[\frac{z}{L}\right]^{d^*}+\cdots\right], \qquad (1.3)$$

where $m_{\infty/2}(z)$ is given by Eq. (1.1) and $d^*=3$ in three dimensions. The value of the constant B depends on the boundary conditions at both the near and the far wall, where the latter can be characterized by a second surface field [10] or by a different boundary condition. Scaling theory does not reveal the form of the correction displayed in Eq. (1.3). The first derivation of Eq. (1.3) was based on the postulate that the total free energy of a film at criticality can be expressed by a *local free energy functional* [10,12], which upon minimization yields Eq. (1.3) with $d^*=(2-\alpha)/\nu$. If hyperscaling holds, then the exponent d^* of the distant wall correction coincides with the spatial dimension d. The structure of the distant wall correction displayed in Eq. (1.3) has been confirmed in $d=2$ for an Ising strip [14] and within the framework of conformal field theory [15], where it turns out that the coefficient B is closely related to the *Casimir amplitude* Δ [16]. In spatial dimensions $d=4-\varepsilon$ near the upper critical dimension $d_c=4$ of simple critical points, Eq. (1.3) has been studied within the framework of the field-theoretic renormalization group within which the exponent relation $d^*=d$ has been confirmed [11,17] and the *short-distance expansion* of scaling operators near one wall has been analyzed in order to obtain the general structure of the corresponding distant wall corrections [18–20]. Thus the close relationship between B and Δ holds also in $d=4-\varepsilon$. A detailed account of the short-distance expansion and the resulting distant wall corrections is given in Ref. [20] so we refrain from discussing any details here.

In the following we will focus on the global aspect of wall effects on scaling density profiles in critical films, i.e., we will study the influence of boundary conditions on the whole *shape* of the profile. In two-dimensional systems at the bulk critical point the principle of conformal invariance can be used in order to obtain scaling density profiles in critical strips from the corresponding simpler profiles in semi-infinite geometries. A semi-infinite geometry with a homogeneous or uniform boundary condition can be mapped onto a strip with equal boundary conditions by means of the *conformal* transformation $\zeta=(L/\pi)\ln\eta$, where $\text{Im}\eta\geq 0$ (upper half plane) and $0\leq\text{Im}\zeta\leq L$. The principle of *conformal invariance* establishes a generalized scaling relation among cumulants of primary scaling operators [15,21] in these two geometries. For a single scalar primary scaling operator $\Psi(\zeta,\bar{\zeta})$ with $\zeta=r_\parallel+iz$ one finds [15,21,22]

$$\langle\Psi(\zeta,\bar{\zeta})\rangle_{\text{strip}}=|\eta'(\zeta)|^{x_\Psi}\langle\Psi(\eta,\bar{\eta})\rangle_{\infty/2}, \qquad (1.4)$$

where the scaling exponent $x_\Psi=\frac{1}{8}$ for the order parameter and $x_\Psi=1$ for the energy density in the Ising universality class. The scaling density profiles in the upper half plane with a homogeneous boundary condition along the real axis can be written as $\langle\Psi(\eta,\bar{\eta})\rangle_{\infty/2}=A_\Psi[(\eta-\bar{\eta})/2i]^{-x_\Psi}$, which follows from pure scaling arguments. The amplitude A_Ψ is nonuniversal and depends on the scaling operator Ψ. From Eq. (1.4) the corresponding scaling density profile in a strip with *equal* boundary conditions can be inferred as [22]

$$\langle\Psi(\zeta,\bar{\zeta})\rangle_{\text{strip}}=A_\Psi\left[\frac{L}{\pi}\sin\frac{\pi z}{L}\right]^{-x_\Psi}, \qquad (1.5)$$

where $z=(\zeta-\bar{\zeta})/2i$. Note that Eq. (1.5) confirms Eq. (1.3) for *any* scaling operator Ψ in $d=2$ for strips with equal boundary conditions.

Strips with *different* boundary conditions a and b along the two edges, respectively, can be represented as conformal images of the upper complex half plane with a boundary condition of type a along the positive real axis and a boundary condition of type b along the negative real axis. The scaling density profile of an operator Ψ in such a half plane reads [16,23]

$$\langle\Psi(\eta,\bar{\eta})\rangle_{a,b,\infty/2}=\left[\frac{\eta-\bar{\eta}}{2i}\right]^{-x_\Psi}F_{ab}^{\Psi}\left[\frac{\eta+\bar{\eta}}{2\sqrt{\eta\bar{\eta}}}\right], \qquad (1.6)$$

where the function F_{ab}^{Ψ} follows from a generalized conformal Ward identity that explicitly depends on the combination (a,b) of the boundary conditions [16]. The boundary conditions a and $b \neq a$ can be combined in two independent ways, namely, $(a,b)=(+,-)$ or $(+,\mathcal{O})$, where $+$ and $-$ denote a *fixed* spin-up and a spin-down boundary condition, respectively, and $\mathcal{O}$ denotes a free boundary condition. A boundary condition of type $+$ or $-$ corresponds to the *extraordinary* surface universality class and a boundary condition of type $\mathcal{O}$ corresponds to the *ordinary* surface universality class (see Sec. II). From Eqs. (1.4) and (1.6) one finds for the order parameter profile $m_{a,b}(z)$ in an Ising strip [16,23]

$$\begin{aligned} m_{+,-}(z) &= A_m \left[\frac{L}{\pi}\sin\frac{\pi z}{L}\right]^{-1/8} \cos\frac{\pi z}{L} , \\ m_{+,\mathcal{O}}(z) &= A_m \left[\frac{L}{\pi}\sin\frac{\pi z}{L}\right]^{-1/8} \left[\cos\frac{\pi z}{2L}\right]^{1/2} . \end{aligned} \tag{1.7}$$

A corresponding analysis can be performed for the energy density profiles $e_{a,b}(z)$ giving [16]

$$\begin{aligned} e_{+,-}(z) &= A_e \left[\frac{L}{\pi}\sin\frac{\pi z}{L}\right]^{-1} \left[1-4\sin^2\frac{\pi z}{L}\right] , \\ e_{+,\mathcal{O}}(z) &= A_e \left[\frac{L}{\pi}\sin\frac{\pi z}{L}\right]^{-1} \cos\frac{\pi z}{L} . \end{aligned} \tag{1.8}$$

More recent results for the energy density profile for $O(N)$ symmetric systems confined to strips in $d=2$ with more combinations of boundary conditions can be found in Ref. [24].

A third set of profiles arises for the Potts magnetization in a two-dimensional strip for various boundary conditions [16]. The profiles given by Eqs. (1.5), (1.7), and (1.8) give a first impression of the global structure of scaling density profiles in critical films and the impact of changing the boundary conditions. We will return to this point in Sec. V. Note that the above examples, except $m_{+,\mathcal{O}}(z)$ for $z \to L$, confirm Eq. (1.3) in $d=2$.

For our field-theoretic analysis in $d=4-\varepsilon$ we use the energy density profile as a paradigm for scaling density profiles in films at bulk criticality [19]. The energy density has the advantage that, in contrast to the order parameter, it has a nonvanishing profile of $T=T_{c,b}$ in the absence of symmetry-breaking surface fields, which allows us to study the symmetry-conserving boundary conditions that will be introduced in Sec. II. After a general discussion of the renormalized energy density profile in Sec. III the energy density profiles for symmetry-conserving boundary conditions at $T=T_{c,b}$ and their corresponding universal scaling functions are presented in Sec. IV. In Sec. V we compare our profiles with results in $d=2$ and discuss the influence of the boundary conditions in detail. A brief account of the short-distance behavior of the profiles is given in Sec. VI and our results are summarized in Sec. VII. Technical details of the calculations are described in Appendixes A–D.

II. MODEL

Within the framework of the field-theoretic renormalization group the so-called Φ^4 Ginzburg-Landau Hamiltonian and suitably augmented forms thereof represent the fixed-point Hamiltonian for systems near critical points. Apart from bulk systems [1,2], this has been shown for semi-infinite systems [5] and in particular for systems confined to regular finite geometries such as, e.g., films [25–28] or cubes [28–30]. The following considerations are devoted to an $O(N)$-symmetric Φ^4 Ginzburg-Landau Hamiltonian in a *film* geometry.

For $O(N)$-symmetric models the order parameter field $\mathbf{\Phi}=(\phi_1,\ldots,\phi_N)$ is a real N-component vector. In particular the values $N=1$, 2, and 3, which correspond to the Ising, the XY, and the Heisenberg universality classes [1,2], respectively, are most relevant for actual experimental systems [see Refs. [10,13] for binary liquid mixtures at the critical demixing points ($N=1$) and Ref. [28] for ^{4}He near $T_\lambda(N=2)$]. The film geometry consists of two parallel plane walls each of area $A \gg L^2$ separated by a distance L with the critical system confined in between. L is considered to be large compared to microscopic lengths. In the spirit of the field-theoretic renormalization group each of the two surfaces of the critical system is characterized by *surface* scaling fields, where the *surface field* $\mathbf{h}_1$ and the *surface enhancement* c, which couple to $\mathbf{\Phi}$ and $\mathbf{\Phi}^2$ at the surface, respectively, are the most relevant ones [5]. Other surface scaling fields such as cubic surface fields w lead to corrections to scaling near the common fixed point $w=0$ [7] and will therefore not be considered here. The Ginzburg-Landau Hamiltonian for a critical film then has the form

$$\begin{aligned} \mathcal{H}[\mathbf{\Phi}] &= \int d^{d-1}r_\parallel \int_0^L dz \left[\frac{1}{2}[\nabla\mathbf{\Phi}(\mathbf{r}_\parallel,z)]^2+\frac{\tau}{2}\mathbf{\Phi}^2(\mathbf{r}_\parallel,z)+\frac{g}{4!}[\mathbf{\Phi}^2(\mathbf{r}_\parallel,z)]^2-\mathbf{h}\cdot\mathbf{\Phi}(\mathbf{r}_\parallel,z)\right] \\ &\quad + \int d^{d-1}r_\parallel \left[\frac{c_a}{2}\mathbf{\Phi}^2(\mathbf{r}_\parallel,0)-\mathbf{h}_{1,a}\cdot\mathbf{\Phi}(\mathbf{r}_\parallel,0)+\frac{c_b}{2}\mathbf{\Phi}^2(\mathbf{r}_\parallel,L)-\mathbf{h}_{1,b}\cdot\mathbf{\Phi}(\mathbf{r}_\parallel,L)\right] , \end{aligned} \tag{2.1}$$

where $\tau=a(T-T_{c,b})/T_{c,b}$ is the bare reduced temperature with $a>0$ being a nonuniversal constant, $g>0$ is the coupling constant, $\mathbf{h}$ is an external bulk field, and $(\nabla\mathbf{\Phi})^2 \equiv \sum_{i=1}^N(\nabla\phi_i)^2$. The surfaces a and b are characterized by surface enhancements c_a and c_b and surface fields $\mathbf{h}_{1,a}$ and $\mathbf{h}_{1,b}$, respectively. The surface enhancements c_a, c_b can be regarded as local, surface specific shifts of the bulk reduced temperature τ. Likewise, the surface fields $\mathbf{h}_{1,a}, \mathbf{h}_{1,b}$ form localized, surface specific corrections to the bulk field $\mathbf{h}$. The field-theoretic analysis of critical systems with surfaces shows that the Hamiltonian in Eq. (2.1) already resembles its functional form at the renormalization-group fixed points. These fixed points correspond to different *surface universality classes* characterized by the fixed-point values $c=-\infty$, 0, and ∞ of the surface enhancement c [5]. The value $c=-\infty$ characterizes the so-called extraordinary (E) surface universality class, which in particular contains systems with a nonzero surface field $\mathbf{h}_1$ [8,17] so that the phenomenon of *critical adsorption* [7,8] must be described within this universality class. For the field-theoretic analysis of the energy density profiles in a critical film, however, we focus on the ordinary ($\mathcal{O}$) and the *surface-bulk* or *special* (SB) surface universality class, which are characterized by $c=\infty$ and 0, respectively. Note that $\mathbf{h}=\mathbf{h}_{1,a}=\mathbf{h}_{1,b}=\mathbf{0}$ in these cases. The fixed-point value $c=\infty$ corresponds to a Dirichlet (D) boundary condition imposed on the order parameter field $\mathbf{\Phi}(\mathbf{r}_\parallel,z)$ with respect to z at the surface. Within mean-field theory $c=0$ corresponds to a Neumann (N) boundary condition. For the film geometry discussed here the $\mathcal{O}$ and the SB surface universality classes can be combined to $(a,b)=(\mathcal{O},\mathcal{O}),(\mathcal{O},SB),(SB,\mathcal{O})$, and (SB,SB), i.e., one has the following combinations of D and N boundary conditions for $\mathbf{\Phi}(\mathbf{r}_\parallel,z)$

$$\begin{aligned}
&c_a=\infty,\quad c_b=\infty \Longleftrightarrow \mathbf{\Phi}(\mathbf{r}_\parallel,0)=\mathbf{\Phi}(\mathbf{r}_\parallel,L)=\mathbf{0}\quad (D-D)\;,\\
&c_a=\infty,\quad c_b=0 \Longleftrightarrow \mathbf{\Phi}(\mathbf{r}_\parallel,0)=\frac{\partial\mathbf{\Phi}}{\partial z}(\mathbf{r}_\parallel,L)=0\quad (D-N)\;,\\
&c_a=0,\quad c_b=\infty \Longleftrightarrow \frac{\partial\mathbf{\Phi}}{\partial z}(\mathbf{r}_\parallel,0)=\mathbf{\Phi}(\mathbf{r}_\parallel,L)=0\quad (N-D)\;,\\
&c_a=0,\quad c_b=0 \Longleftrightarrow \frac{\partial\mathbf{\Phi}}{\partial z}(\mathbf{r}_\parallel,0)=\frac{\partial\mathbf{\Phi}}{\partial z}(\mathbf{r}_\parallel,L)=0\quad (N-N)\;.
\end{aligned}\tag{2.2}$$

Note that the combination $N-D$ of boundary conditions is equivalent to the combination $D-N$ applied to $\mathbf{\Phi}(\mathbf{r}_\parallel,L-z)$ at $z=0,L$. Furthermore, we note that the SB surface universality class (N boundary condition) corresponds to a *multicritical* point, which is located at $c=0$ only within the *dimensional* regularization scheme [1], which we adopt for the calculation of the energy density profiles. Beyond mean-field theory fluctuations destroy the equivalence of the condition $c=0$ and the Neumann boundary condition for the order parameter (see Ref. [5]).

In contrast to the E surface universality class, which is characterized by a *symmetry-breaking* surface field, the boundary conditions in Eq. (2.2) that are associated with the $\mathcal{O}$ and SB surface universality classes can be regarded as *symmetry conserving.* If surface contributions to the Hamiltonian given by Eq. (2.1) are absent, periodic and antiperiodic boundary conditions are considered as a second set of symmetry-conserving boundary conditions. The order parameter in this case has the properties

$$\mathbf{\Phi}(\mathbf{r}_\parallel,z)=\begin{cases}\mathbf{\Phi}(\mathbf{r}_\parallel,z+L) & \text{(periodic)}\\ -\mathbf{\Phi}(\mathbf{r}_\parallel,z+L) & \text{(antiperiodic),}\end{cases}\tag{2.3}$$

respectively. The free propagators $G_{ij}^{(0)a,b}(\mathbf{p},\mathbf{p}';z,z')$ fulfill the boundary conditions listed in Eqs. (2.2) and (2.3) with respect to the perpendicular coordinates z and z'. Their explicit form is given in Appendix B.

III. RENORMALIZED ENERGY DENSITY PROFILE

In the vicinity of a bulk critical point the internal energy $\mathcal{U}(T,L)$ of a film measured in units of $k_BT_{c,b}$ and per area A can be decomposed into a regular part $u^{\text{reg}}(t,L)$ and a singular part $u^{\text{sing}}(t,L)$ as functions of the reduced temperature t (see below) and the film thickness L according to

$$\lim_{A\to\infty}\frac{\mathcal{U}(T,L)}{k_BT_{c,b}A}=u^{\text{reg}}(t,L)+u^{\text{sing}}(t,L)\;.\tag{3.1}$$

In the following we will refer to u^{reg} and u^{sing} as the regular and the singular *energy density* per area, respectively. Using the thermodynamical relation $\mathcal{U}=-T^2\partial/\partial T(\mathcal{F}/T)$ between the internal energy $\mathcal{U}$ and the free energy $\mathcal{F}$ of the film, the regular and the singular energy density can be related to the regular and the singular part of the free energy density, respectively. The singular contribution to thermodynamic functions can be obtained from the *renormalized* field-theoretic model described in Sec. II. The renormalization procedure for the free energy density has already been described in Ref. [26] in great detail so that here we present only the conclusions for the singular part $u^{\text{sing}}(t,L)$ of the energy density. First, we define a *bare* energy density $\bar{u}(\tau,L)$ for the field-theoretic model in Eq. (2.1) by

$$\bar{u}(\tau,L)=-\frac{1}{2}\int_0^L\langle\mathbf{\Phi}^2(\mathbf{r}_\parallel,z)\rangle dz\;,\tag{3.2}$$

which is in accordance with the thermodynamical relation

$$\bar{u}(\tau,L)=-\frac{\partial}{\partial\tau}\bar{f}(\tau,L)\;,\tag{3.3}$$

where $\bar{f}(\tau,L)$ is the bare free energy density defined in Ref. [26]. Note that the thermal average $\langle\mathbf{\Phi}^2(\mathbf{r}_\parallel,z)\rangle$ with respect to $\mathcal{H}$ given by Eq. (2.1) does not depend on $\mathbf{r}_\parallel$. For simplicity the dependence of $\bar{u}$ and $\bar{f}$ on the bare coupling constant g has been dropped in Eqs. (3.2) and (3.3). In the absence of external fields the renormalized thermodynamical functions, which give access to the singular thermodynamical behavior of the system, are only functions of the renormalized reduced temperature t and the renormalized coupling constant u, which are given by

$$\tau=\mu^2Z_tt,\quad g=2^d\pi^{d/2}\mu^{\varepsilon}Z_uu\tag{3.4}$$

within the dimensional regularization scheme, where $\varepsilon=4-d$, Z_t and Z_u are the usual bulk renormalization factors [1,2], and μ is an arbitrary momentum scale. In accordance with Eq. (3.3) we define the renormalized energy density $u^R(t,L)$ by

$$u^R(t,L)=-\frac{\partial}{\partial t}f^R(t,L)\;,\tag{3.5}$$

where in a simplified notation $f^R(t,L)=\bar{f}(\tau,L)-\bar{f}(\tau_1,L)-\bar{f}_\tau(\tau_1,L)(\tau-\tau_1)-\frac{1}{2}\bar{f}_{\tau\tau}(\tau_1,L)(\tau-\tau_1)^2$ denotes the renormalized free energy density as defined in Ref. [26]. From Eq. (3.5) we therefore have the explicit renormalization prescription

$$u^R(t,L)=\mu^2 Z_t[\bar{u}(\tau,L)-\bar{u}(\tau_1,L)-\bar{u}_\tau(\tau_1,L)(\tau-\tau_1)] \tag{3.6}$$

for the renormalized energy density in terms of the bare energy density $\bar{u}$ [see Eq. (3.2)] and its first derivative $\bar{u}_\tau$ with respect to τ. Besides the multiplicative renormalization by Z_t the energy density requires two subtractions taken at a reference value τ_1 of the bare reduced temperature τ, which we choose according to

$$\tau_1=\mu^2 Z_t \operatorname{sgn} t \tag{3.7}$$

(see Ref. [26]). Note that the subtractions in Eq. (3.6) form a Taylor polynomial of first degree for the bare energy density at the reference point τ_1. Besides containing the critical singularities $u^R(t,L)$ therefore fulfills the *normalization conditions*

$$u^R(\operatorname{sgn},L)=0, \quad u_t^R(\operatorname{sgn} t,L)=0 \; . \tag{3.8}$$

In order to simplify the notation we will identify $u^{\text{sing}}(t,L)$ in Eq. (3.1) with the renormalized energy density $u^R(t,L)$ in the following.

In a second step we define a *bare energy density profile* $\bar{e}(\tau,z,L)$ by

$$\bar{e}(\tau,z,L)=-\tfrac{1}{2}\langle \mathbf{\Phi}^2(\mathbf{r}_\parallel,z)\rangle \tag{3.9}$$

so that the bare energy density $\bar{u}(\tau,L)$ is the integral over $\bar{e}(\tau,z,L)$ with respect to z within the dimensional regularization scheme used here [see Eq. (3.2)]. The renormalized energy density can then be represented in the form

$$u^R(t,L)=\int_0^L e^R(t,z,L)dz \; , \tag{3.10}$$

where the *renormalized energy density profile* $e^R(t,z,L)$ is related to the bare energy density profile $\bar{e}(\tau,z,L)$ by applying the renormalization prescription for $\bar{u}(\tau,L)$ [see Eq. (3.6)] directly to $\bar{e}(\tau,z,L)$. One therefore has

$$e^R(t,z,L)=\mu^2 Z_t[\bar{e}(\tau,z,L)-\bar{e}(\tau_1,z,L) -\bar{e}_\tau(\tau_1,z,L)(\tau-\tau_1)] \tag{3.11}$$

so that $e^R(t,z,L)$ fulfills the same normalization conditions as $u^R(t,L)$ [see Eq. (3.8)]. The renormalization prescription in Eq. (3.11) differs from the prescription for the renormalized energy density profile in a semi-infinite system given in Ref. [6] only with respect to the prefactor μ^2. The renormalized energy density profile $e^R(t,z,L)$ in Eq. (3.11) has a *finite* limit as $z\rightarrow 0$ or L because the limit $z\rightarrow 0$ in Eq. (3.11) first means that z becomes very small compared to L, but remains large compared to any *microscopic* length. Therefore the renormalized energy density profile $e^R(t,z,L)$ in the film approaches its counterpart $e^R_{\infty/2}(t,z)$ in a semi-infinite geometry that remains finite as z is further reduced to zero [6]. By the same reasoning $e^R(t,z,L)$ approaches a finite value as $z\rightarrow L$ because in this case $z'=L-z$ becomes small compared to L. From the short discussion after Eq. (1.1) one may come to the conclusion that $e^R(t,z,L)$ contains a microscopic length scale that manages the crossover to a finite value as $z\rightarrow 0$ or L. This is in fact the case because instead of the reduced temperature t, the bulk correlation length $\xi_\pm(t)=\xi_0^\pm|t|^{-\nu}$ can serve as the third argument in $e^R(t,z,L)$. If one defines

$$e(t,z,L)=\mu^2 Z_t \bar{e}(\tau,z,L) \tag{3.12}$$

as a multiplicatively renormalized energy density profile that does not fulfill the normalization conditions given by Eq. (3.8), $e^R(t,z,L)$ can be written in the form

$$e^R(t,z,L)=e(t,z,L)-e(\operatorname{sgn} t,z,L) -e_t(\operatorname{sgn} t,z,L)(t-\operatorname{sgn} t) \; . \tag{3.13}$$

After changing the variables according to $e(t,z,L)\equiv\tilde{e}(\xi_\pm,z,L)$, the corresponding renormalized energy density profile $\tilde{e}^R(\xi_\pm,z,L)$ contains the same subtractions as in Eq. (3.13), which depend on the microscopic correlation length *amplitude* $\xi_0^\pm=\xi_\pm(t_1=\operatorname{sgn} t)$ according to

$$\tilde{e}^R(\xi_\pm,z,L)=\tilde{e}(\xi_\pm,z,L)-\tilde{e}(\xi_0^\pm,z,L) +\nu\xi_0^\pm\tilde{e}_{\xi_\pm}(\xi_0^\pm,z,L)[(\xi_\pm/\xi_0^\pm)^{-1/\nu}-1] \; . \tag{3.14}$$

The desired microscopic scale is therefore set by $\xi_0^\pm$. The profile $e(t,z,L)=\tilde{e}(\xi_\pm,z,L)$, however, only depends on the *macroscopic* lengths as indicated by the arguments. In the limit $z\rightarrow 0$ (i.e., $z\ll L$) $e(t,z,L)$ approaches its counterpart in a semi-infinite geometry (see Ref. [6]), which is of the form indicated by Eq. (1.2). Therefore $e(t,z,L)$ *diverges* like $z^{-(1-\alpha)/\nu}$ as $z\rightarrow 0$ and like $(L-z)^{-(1-\alpha)/\nu}$ as $z\rightarrow L$.

We use the remainder of this section to show that the renormalized energy density profile can be represented by a *universal* scaling function. The main argument for this statement can be obtained from the solution of the renormalization-group equations (RGEs) for $e^R(t,z,L)$, which are given by [6]

$$\left[\mu\frac{\partial}{\partial\mu}+\beta(u)\frac{\partial}{\partial u}-\frac{t}{\nu(u)}\frac{\partial}{\partial t}-\frac{3}{\nu(u)}\right]e_{tt}^R=0 \; ,$$

$$\left[\mu\frac{\partial}{\partial\mu}+\beta(u)\frac{\partial}{\partial u}-\frac{t}{\nu(u)}\frac{\partial}{\partial t}-\frac{1}{\nu(u)}\right]e^R = -\frac{t-\operatorname{sgn} t}{\nu(u)}e_{tt}^R|_{t=\operatorname{sgn} t} \tag{3.15}$$

(see also Ref. [26]), where $\beta(u)$ and $\nu(u)$ are the standard Wilson functions [1,2]. Note that the macroscopic lengths z and L are not renormalized and therefore they do not occur in Eq. (3.15). Using the method of characteristics the RGEs can be solved straightforwardly and we refer to Sec. III of Ref. [26] for details. With the well-known nonuniversal fixed-point amplitude factor

$$E_\nu^*(u)=\int_u^{u^*}\left[\frac{1}{\nu}-\frac{1}{\nu(u)}\right]\frac{du}{\beta(u)} \tag{3.16}$$

we have for $e_{tt}^R(t,z,L)$ the fixed-point solution

$$e_{tt}^R(t,z,L)=L^{-d}(\mu L)^{1/\nu}E_\nu^*(u) \times\frac{\partial^2}{\partial t^2}h_\pm(E_\nu^*(u)(\mu L)^{1/\nu}|t|,z/L) \quad (3.17)$$

[see Eq. (3.13) in Ref. [26]], where u^* is the infrared stable renormalization-group fixed point $\beta(u^*)=0$ and $\nu=\nu(u^*)$. The prefactor L^{-d} yields the correct naive dimension for the energy density profile, which according to Eqs. (3.1) and (3.10) is given by an inverse volume. The scaling functions $h_+(w,x)$ for $t>0$ and $h_-(w,x)$ for $t<0$ are left undetermined by the RGEs. The scaling arguments w and x are defined by

$$w=E_\nu^*(u)(\mu L)^{1/\nu}|t|, \quad x=z/L \ . \quad (3.18)$$

According to Eq. (3.17) the renormalized energy density profile $e^R(t,z,L)$ has the fixed-point form [see also Eq. (3.16) in Ref. [26]]

$$e^R(t,z,L)=L^{-d}(\mu L)^{1/\nu}E_\nu^*(u)\left[h_\pm(w,x)-h_\pm(w_1,x) -\frac{\partial h_\pm}{\partial w}(w_1,x)(w-w_1)\right], \quad (3.19)$$

where the reference value w_1 of the scaling variable w is given by $w_1=(\mu L)^{1/\nu}E_\nu^*(u)$. Accordingly, the multiplicatively renormalized energy density profile $e(t,z,L)$ [see Eq. (3.12)] is given by

$$e(t,z,L)=L^{-d}(\mu L)^{1/\nu}E_\nu^*(u)h_\pm(w,x) \quad (3.20)$$

at the renormalization-group fixed point. The amplitude factor $E_\nu^*(u)$ given by Eq. (3.16) is nonuniversal because it depends on the renormalized coupling constant u, which in turn is a function of the microscopic parameters of the system and is therefore nonuniversal itself. However, the u dependence of $e^R(t,z,L)$ is completely absorbed in the amplitude factor $E_\nu^*(u)$, which appears only in the scaling argument w and in the prefactor of the profile. The *functions* $h_\pm$ do *not* depend on u, i.e., they are universal.

For short-ranged interactions and within the Ising universality class ($N=1$) the scaling argument w can be expressed in terms of the bulk correlation length $\xi_\pm=\xi_0^\pm|t|^{-\nu}$. The aforementioned conditions allow one to adopt the definition of $\xi_\pm$ via the second moment of the bulk two-point correlation function $G_\pm(\mu,x,|t|,u)$ according to

$$\xi_\pm^2=\frac{1}{2d}\frac{\int d^dx\, x^2G_\pm(\mu,x,|t|,u)}{\int d^dx\, G_\pm(\mu,x,|t|,u)} \quad (3.21)$$

[see Eq. (4.2) in Ref. [26]], which implies [see Eq. (4.5) in Ref. [26]]

$$\xi_0^\pm=\left[\frac{k_\pm}{2d}\right]^{1/2}\mu^{-1}[E_\mu^*(u)]^{-\nu} \quad (3.22)$$

for the correlation length amplitude $\xi_0^\pm$, where $k_\pm$ is a universal constant. Defining a scaling argument $y_\pm=L/\xi_\pm$ and a universal scaling function $\tilde{h}_\pm(y_\pm,x)$, Eq. (3.20) can be rewritten according to

$$\begin{aligned} e(t,z,L)&=\tilde{e}(\xi_\pm,z,L)\\ &=L^{-d}\left[\frac{L}{\xi_0^\pm}\right]^{1/\nu}\left[\frac{k_\pm}{2d}\right]^{1/(2\nu)} \times h_\pm\left[\left[\frac{k_\pm}{2d}\right]^{1/(2\nu)}\left[\frac{L}{\xi_\pm}\right]^{1/\nu},\frac{z}{L}\right]\\ &\equiv L^{-d}\left[\frac{L}{\xi_0^\pm}\right]^{1/\nu}\tilde{h}_\pm(y_\pm,x)\ . \end{aligned} \quad (3.23)$$

Note that, unlike $h_\pm$, the scaling functions $\tilde{h}_\pm$ depend on the definition of the correlation length $\xi_\pm$. Finally, the renormalized energy density profile $\tilde{e}^R(\xi_\pm,z,L)$ [see Eq. (3.14)] has the representation

$$\tilde{e}^R(\xi_\pm,z,L)=L^{-d}\left[\frac{L}{\xi_0^\pm}\right]^{1/\nu}\left[\tilde{h}_\pm(y_\pm,x)-\tilde{h}_\pm(y_{1\pm},x)-\nu\frac{\partial\tilde{h}_\pm}{\partial y_\pm}(y_{1\pm},x)y_{1\pm}^{1-1/\nu}(y_\pm^{1/\nu}-y_{1\pm}^{1/\nu})\right], \quad (3.24)$$

where $y_{1\pm}=L/\xi_0^\pm$.

As we restrict our discussion of the energy density profiles to the case $t=0$ from the beginning we are not able to evaluate Eq. (3.11). Therefore we resort to Eq. (3.12), which yields the multiplicatively renormalized energy density profile $e(0,z,L)$ and the scaling function $h_\pm(0,x)$ or $\tilde{h}_\pm(0,x)$, respectively [see Eqs. (3.20) and (3.23)]. In view of our main objective, the restriction to Eq. (3.12) poses of course no limitation on the possible choice of the boundary conditions so that $e^R(0,z,L)$ and $e(0,z,L)$ are equally well suited for our purposes. Finally, we note that even for the investigation of distant wall corrections the different behavior of $e^R(0,z,L)$ and $e(0,z,L)$ for $z\to 0$ is irrelevant because within continuum theory the coordinate z is always much larger than any microscopic length scale so that, although $z \ll L$ in this case, one is still far away from the limit $z\to 0$.

IV. SCALING FUNCTIONS AT BULK CRITICALITY

The energy density profiles $\overline{e}(\tau,z,L)$, $e(t,z,L)$, and $e^R(t,z,L)$ defined in Sec. III depend on the combination (a,b) of boundary conditions at the surfaces ($z=0,L$) of the film. We keep track of this dependence by assigning the subscript a,b to the energy density profiles in the fol-

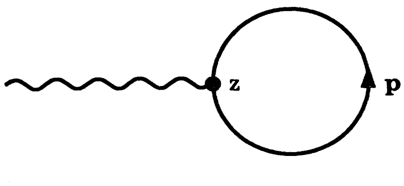

FIG. 1. One-loop Feynman diagram for the bare energy density profile $\bar{e}(\tau,z,L)$. The momentum **p** running in the loop corresponds to the parallel momentum in the spectral representation of the Hamiltonian [see Eqs. (B1) and (B2)]. The coordinate z indicates the position between the plates where $\bar{e}_{a,b}$ is evaluated.

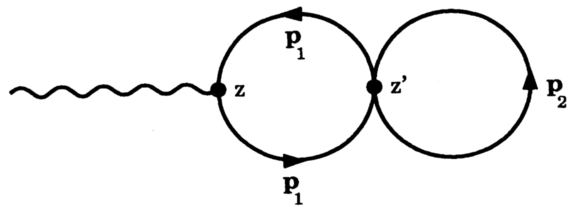

FIG. 2. Two-loop Feynman diagram for the bare energy density profile $\bar{e}(\tau,z,L)$. The coordinate z indicates the position of $\bar{e}_{a,b}$. Integrations must be performed over the momenta $\mathbf{p}_1$ and $\mathbf{p}_2$ and over the vertex position z'. The combinatorial factor of this diagram is 12.

lowing.

In order to obtain a field-theoretic approximation for $e_{a,b}(t=0,z,L)$ [see Eq. (3.12)] we first determine the bare energy density profile $\bar{e}_{a,b}(\tau=0,z,L)$ from Eqs. (2.1) and (3.9) to first-order perturbation theory in the bare coupling constant g. The propagators and vertices needed to facilitate the perturbation expansion in terms of Feynman diagrams are listed in Eqs. (B4)–(B9) in Appendix B for all boundary conditions under consideration [see Eqs. (2.2) and (2.3)]. To leading order the energy density profiles are given by the one-loop diagram shown in Fig. 1. According to the standard Feynman rules [1,2], the analytic expression that corresponds to Fig. 1 in the case of O(N) symmetry is given by

$$\bar{e}^{(1)}_{a,b}(\tau,z,L)=-\frac{N}{2}\int\frac{d^{d-1}p}{(2\pi)^{d-1}}G^{(0)a,b}(\mathbf{p};z,z)\ , \qquad (4.1)$$

where the Green's functions $G^{(0)a,b}(\mathbf{p};z,z')$ are defined by Eq. (C2) in Appendix C for $\tau\geq 0$. The $(d-1)$-dimensional integration over the parallel momentum **p** in Eq. (4.1) can most conveniently be performed using the dimensional regularization scheme (see, e.g., Ref. [1]). For $\tau=0$ a detailed derivation of the one-loop contributions $\bar{e}^{(1)}_{a,b}(0,z,L)$ to the bare energy density profiles is presented in Appendix C, which the reader should consult for the implementation of the dimensional regularization scheme in this case. At the upper critical dimension $d=d_c=4$ the one-loop profiles derived in Appendix C can be regarded as exact.

The first-order correction to the bare energy density profile is given by the two-loop Feynman diagram shown in Fig. 2. The coordinate z indicates the position between the plates where the profile is evaluated and z' indicates the position of the vertex, which must be integrated over the interval $[0,L]$. The parallel momentum labels $\mathbf{p}_1$ and $\mathbf{p}_2$ already account for momentum conservation at the vertex [see Eq. (B9)]. According to the standard Feynman rules, Fig. 2 corresponds to the expression

$$\bar{e}^{(2)}_{a,b}(\tau,z,L)=gN\frac{N+2}{12}\int_0^L dz'\int\frac{d^{d-1}p_1}{(2\pi)^{d-1}}[G^{(0)a,b}(\mathbf{p}_1;z,z')]^2\times\int\frac{d^{d-1}p_2}{(2\pi)^{d-1}}G^{(0)a,b}(\mathbf{p}_2;z',z') \qquad (4.2)$$

for the O(N)-symmetric Hamiltonian given by Eq. (2.1). However, the evaluation of Eq. (4.2) turns out to be a major task even in the case $\tau=0$ on which we focus here. A guideline of how to extract the ε expansion of $\bar{e}^{(2)}_{a,b}(0,z,L)$ from the integrals in Eq. (4.2) is given in Appendix D, where the dimensional regularization scheme has been applied throughout the calculation.

Using the results from Appendixes C and D the multiplicative renormalization prescription in Eq. (3.12) can be carried out with the well-known *bulk* renormalization Z factors [1,2]

$$Z_t=1+\frac{N+2}{3}\frac{u}{\varepsilon}+O(u^2),\quad Z_u=1+O(u)\ , \qquad (4.3)$$

which yield the representation

$$e_{a,b}(0,z,L)=\mu^2[Z_t\bar{e}^{(1)}_{a,b}(0,z,L)+\bar{e}^{(2)}_{a,b}(0,z,L)+O(u^2)] \qquad (4.4)$$

to two-loop order. At the renormalization-group fixed point [1,2]

$$u^*=\frac{3\varepsilon}{N+8}+O(\varepsilon^2) \qquad (4.5)$$

one obtains the ε expansions for $\bar{e}_{a,b}(0,z,L)$ in $d=4-\varepsilon$. For equal boundary conditions we find

$$e_{\mathcal{O},\mathcal{O}}(0,z,L)=\frac{N}{2}\frac{\Gamma\left[\frac{d}{2}-1\right]}{2^d\pi^{d/2}}L^{-d}(\mu L)^2\left\{\frac{\pi^2}{\sin^2\pi x}-\frac{\pi^2}{3}-\varepsilon\left[\zeta'(2,x)+\zeta'(2,1-x)-2\zeta'(2)+\frac{N+2}{N+8}\left[\frac{\pi^2}{\sin^2\pi x}-\frac{\pi^2}{3}\right]\left[\frac{C}{2}+\ln\mu L-\ln\frac{\pi}{\sin\pi x}\right]+\frac{1}{2}\frac{N+2}{N+8}\frac{\pi^2}{\sin^2\pi x}\right]+O(\varepsilon^2)\right\} \tag{4.6}$$

and

$$e_{SB,SB}(0,z,L)=-\frac{N}{2}\frac{\Gamma\left[\frac{d}{2}-1\right]}{2^d\pi^{d/2}}L^{-d}(\mu L)^2\times\left\{\frac{\pi^2}{\sin^2\pi x}+\frac{\pi^2}{3}-\varepsilon\left[\zeta'(2,x)+\zeta'(2,1-x)+2\zeta'(2)+\frac{N+2}{N+8}\left[\frac{\pi^2}{\sin^2\pi x}-\frac{\pi^2}{3}\right]\left[\frac{C}{2}+\ln\mu L-\ln\frac{\pi}{\sin\pi x}\right]-\frac{1}{2}\frac{N+2}{N+8}\frac{\pi^2}{\sin^2\pi x}-\frac{2\pi^2}{3}\frac{N+2}{N+8}\left[\ln 2\pi-\frac{C}{2}-3-\ln\mu L\right]\right]+O(\varepsilon^2)\right\}, \tag{4.7}$$

where $x=z/L, C=0.577\,216\,6\ldots$ is Euler's constant, and $\zeta'(\alpha,x)=(\partial/\partial\alpha)\zeta(\alpha,x)$ (see Appendix A). The energy density profile for mixed boundary conditions is given by

$$e_{\mathcal{O},SB}(0,z,L)=\frac{N}{2}\frac{\Gamma\left[\frac{d}{2}-1\right]}{2^d\pi^{d/2}}L^{-d}(\mu L)^2\times\left[\frac{\pi^2\cos\pi x}{\sin^2\pi x}+\frac{\pi^2}{6}-\varepsilon\left\{\eta'(2,x)-\eta'(2,1-x)+2\eta'(2)+\frac{N+2}{N+8}\left[\frac{\pi^2\cos\pi x}{\sin^2\pi x}+\frac{\pi^2}{6}\right]\left[\frac{C}{2}+\ln\mu L-\ln\frac{\pi}{\sin\pi x}\right]+\frac{1}{2}\frac{N+2}{N+8}\frac{\pi^2}{\sin^2\pi x}+\frac{\pi^2}{6}\frac{N+2}{N+8}\left[\ln\frac{\pi}{\sin\pi x}-\ln\left[\frac{\pi}{2}\cot\frac{\pi}{2}x\right]\right]\right\}+O(\varepsilon^2)\right], \tag{4.8}$$

where $\eta'(\alpha,x)=(\partial/\partial\alpha)\eta(\alpha,x)$ (see Appendix A). Note that $e_{SB,\mathcal{O}}(0,z,L)=e_{\mathcal{O},SB}(0,L-z,L)$. In the absence of free surfaces periodic

$$e_{\rm per}(0,z,L)=-N\frac{\Gamma\left[\frac{d}{2}-1\right]}{\pi^{d/2}}L^{-d}\left[\frac{\mu L}{2}\right]^2\left\{\frac{\pi^2}{6}-\varepsilon\left[\zeta'(2)+\frac{\pi^2}{6}\frac{N+2}{N+8}\left[\frac{C}{2}-\ln 2\pi+\ln\frac{\mu L}{2}\right]\right]+O(\varepsilon^2)\right\} \tag{4.9}$$

and antiperiodic boundary conditions

$$e_{\rm aper}(0,z,L)=N\frac{\Gamma\left[\frac{d}{2}-1\right]}{\pi^{d/2}}L^{-d}\left[\frac{\mu L}{2}\right]^2\left\{\frac{\pi^2}{12}-\varepsilon\left[\eta'(2)+\frac{\pi^2}{12}\frac{N+2}{N+8}\left[\frac{C}{2}-\ln\frac{\pi}{2}+\ln\frac{\mu L}{2}\right]\right]+O(\varepsilon^2)\right\} \tag{4.10}$$

yield finite-size effects which are spatially constant. According to the scaling behavior of $e(\tau,z,L)$ shown in Eq. (3.23) the universal scaling functions $\tilde{h}_{+a,b}(0,x)$ can be determined from Eqs. (4.6)–(4.10) due to

$$e_{a,b}(0,z,L)=L^{-d}\left[\frac{L}{\xi_0^+}\right]^{1/\nu}\tilde{h}_{+a,b}(0,x)\ . \tag{4.11}$$

For the identification of the factor $(L/\xi_0^+)^{1/\nu}$ in Eqs. (4.6)–(4.10) we use the ε expansion of the exponent ν [1,2]

$$\frac{1}{\nu}=2-\varepsilon\frac{N+2}{N+8}+O(\varepsilon^2) \tag{4.12}$$

and of the correlation length amplitude ξ_0^+ [31]

$$\xi_0^+=\mu^{-1}\left[1+\frac{\varepsilon}{4}\frac{N+2}{N+8}(1-C)+O(\varepsilon^2)\right] \tag{4.13}$$

in the dimensional regularization scheme. For convenience we furthermore define universal scaling functions $g_{a,b}(x)$ by splitting off a universal amplitude $A_{a,b}$,

$$\tilde{h}_{+a,b}(0,x)\equiv A_{a,b}g_{a,b}(x)\ . \tag{4.14}$$

For $a=b$ the amplitude $A_{a,b}$ is defined by the requirement that $g_{a,b}(x\to 0)=x^{-d+1/\nu}$ so that $A_{a,a}$ is the universal amplitude of the energy density profile $e_{a,\infty/2}(0,z)$ in the limit of a semi-infinite system with a boundary condition of type a, i.e.,

$$e_{a,\infty/2}(0,z)=\lim_{L\to\infty}e_{a,a}(0,z,L)=A_{a,a}z^{-d}\left[\frac{z}{\xi_0^+}\right]^{1/\nu}\ . \tag{4.15}$$

For $a\neq b$ it is convenient to define $A_{a,b}$ such that $g_{b,a}(x)=g_{a,b}(1-x)$ and so that $g_{a,b}(x\to 0)g_{b,a}(x\to 0)=-x^{-2(d-1/\nu)}$, which also implies $A_{a,b}=A_{b,a}$. For periodic and antiperiodic boundary conditions we define the amplitudes $A_{\rm per}$ and $A_{\rm aper}$ by the requirement $g_{\rm per}(x)=g_{\rm aper}(x)=1$. Within the ε expansion we then obtain from Eqs. (4.6)–(4.15), for equal boundary conditions,

$$A_{O,O}=\frac{N}{2}\frac{\Gamma\left[\frac{d}{2}-1\right]}{2^d\pi^{d/2}}\left[1-\varepsilon\frac{N+2}{N+8}C\right]\ , \tag{4.16a}$$

$$g_{O,O}(x)=\left[\frac{\pi^2}{\sin^2\pi x}-\frac{\pi^2}{3}\right]\left[1+\varepsilon\frac{N+2}{N+8}\ln\frac{\pi}{\sin\pi x}\right]-\varepsilon[\zeta'(2,x)+\zeta'(2,1-x)-2\zeta'(2)]-\varepsilon\frac{N+2}{N+8}\frac{\pi^2}{6} \tag{4.16b}$$

and

$$A_{SB,SB}=-A_{O,O}\left[1+\varepsilon\frac{N+2}{N+8}\right]\ , \tag{4.17a}$$

$$g_{SB,SB}(x)=g_{O,O}(x)+4\zeta(2)\left\{1-\varepsilon\left[\frac{\zeta'(2)}{\zeta(2)}+\frac{N+2}{N+8}(3-\ln 2\pi)\right]\right\}\ . \tag{4.17b}$$

For mixed boundary conditions we find

$$A_{O,SB}=A_{O,O}\left[1+\frac{\varepsilon}{2}\frac{N+2}{N+8}\right]=A_{SB,O}\ , \tag{4.18a}$$

$$\begin{aligned}g_{O,SB}(x)&=g_{SB,O}(1-x)\\&=\frac{\pi^2\cos\pi x}{\sin^2\pi x}\left[1+\varepsilon\frac{N+2}{N+8}\ln\frac{\pi}{\sin\pi x}\right]+\frac{\pi^2}{6}\left[1+\varepsilon\frac{N+2}{N+8}\ln\left[\frac{\pi}{2}\cot\frac{\pi}{2}x\right]\right]\\&\quad-\varepsilon[\eta'(2,x)-\eta'(2,1-x)+2\eta'(2)]-\frac{\varepsilon}{2}\frac{N+2}{N+8}\frac{\pi^2}{\sin^2\pi x}\ .\end{aligned} \tag{4.18b}$$

For periodic and antiperiodic boundary conditions one has, for the universal amplitudes,

$$A_{\rm per}=-N\frac{\Gamma\left[\frac{d}{2}-1\right]}{4\pi^{d/2}}\zeta(2)\left\{1-\varepsilon\left[\frac{\zeta'(2)}{\zeta(2)}-\frac{N+2}{N+8}\left[\frac{1}{2}+\ln 4\pi-C\right]\right]\right\} \tag{4.19}$$

and

$$A_{\rm aper}=N\frac{\Gamma\left[\frac{d}{2}-1\right]}{4\pi^{d/2}}\eta(2)\left\{1-\varepsilon\left[\frac{\eta'(2)}{\eta(2)}-\frac{N+2}{N+8}\left[\frac{1}{2}+\ln\pi-C\right]\right]\right\}\ , \tag{4.20}$$

whereas the corresponding scaling functions are constant:

$$g_{\rm per}(x)=g_{\rm aper}(x)=1\ . \tag{4.21}$$

We used the expansion

$$x^{-d+1/\nu}=x^{-(d-2)}\left[1-\varepsilon\frac{N+2}{N+8}\ln x+O(\varepsilon^2)\right].$$

Due to the definition of the amplitude $A_{O,SB}$ the scaling functions $g_{O,SB}(x)$ and $g_{SB,O}(x)$ involve an additional amplitude in their asymptotic behavior for $x\to 0$. From Eq. (4.18b) we obtain

$$g_{O,SB}(x\to 0)=\left[1-\frac{\varepsilon}{2}\frac{N+2}{N+8}\right]x^{-d+1/\nu} \tag{4.22a}$$

and

$$g_{SB,O}(x\to 0)=-\left[1+\frac{\varepsilon}{2}\frac{N+2}{N+8}\right]x^{-d+1/\nu} \tag{4.22b}$$

so that

$$A_{O,O}g_{O,O}(x\to 0)=A_{O,SB}g_{O,SB}(x\to 0)=A_{O,O}x^{-d+1/\nu} \tag{4.23a}$$

and

$$A_{SB,SB}g_{SB,SB}(x\to 0)=A_{SB,O}g_{SB,O}(x\to 0)=A_{SB,SB}x^{-d+1/\nu}\ . \tag{4.23b}$$

In the limit $L\to\infty$ the energy density profiles $e_{a,b}(0,z,L)$ therefore represent the semi-infinite limit $e_{a,\infty/2}(0,z)$ in the form [see Eq. (4.15)]

$$\lim_{L\to\infty}e_{a,b}(0,z,L)=e_{a,\infty/2}(0,z)=A_{a,a}z^{-d}\left[\frac{z}{\xi_0^+}\right]^{1/\nu}, \tag{4.24}$$

where the boundary of type b is always assumed to be located at $z=L$.

V. EXPONENTIATED ENERGY DENSITY PROFILES

Within the ε expansion the scaling functions $g_{a,b}(x)$ contain *logarithmic* contributions that originate from the series representation of functions involving ε-dependent powers such as

$$\left[\frac{\pi}{\sin\pi x}\right]^{\varepsilon}=1+\varepsilon\ln\frac{\pi}{\sin\pi x}+O(\varepsilon^2)\ . \tag{5.1}$$

In order to obtain an approximation for the scaling function $g_{a,b}(x)$ in three dimensions one might simply extrapolate the ε expansion given by Eqs. (4.16a)–(4.21) to $\varepsilon=1$. However, apart from general ambiguities in this approach, in the vicinity of $x=0$ and 1 (i.e., near the surface of the film) the simple extrapolation leads to a gross misrepresentation of the scaling functions, as may already be seen from Eq. (5.1). Although valuable conclusions can be drawn from the ε expansion in Eqs. (4.16a)–(4.21) (see Sec. VI) it is numerically unreliable and therefore useless for an analysis of the global shape of the scaling functions $g_{a,b}(x)$.

In order to find a numerically more reliable representation of $g_{a,b}(x)$ in $d=3$ one can, for example, consider a *resummation* or an *exponentiation* of the ε expansion given by Eqs. (4.16a)–(4.21) that reproduces the limiting behavior of $g_{a,b}(x)$ for $x\to 0$ and 1 correctly [see Eqs. (4.22a) and (4.23b)]. Moreover, the ε expansions of $g_{O,O}(x)$ and $g_{O,SB}(x)$ for small x are consistent with the short-distance behavior displayed in Eq. (1.3), which we will therefore use as another restriction for the exponentiation of Eqs. (4.16a)–(4.21). The short-distance behavior of $g_{SB,SB}(x\to 0)$ and $g_{SB,O}(x)=g_{O,SB}(1-x)$, however, has a different form (see below).

First, we consider $g_{O,O}(x)$, which represents the simplest nontrivial scaling function. Due to the symmetry $g_{O,O}(x)=g_{O,O}(1-x)$, the limiting behavior of $g_{O,O}(x)$ for $x\to 1$ is the same as for $x\to 0$. By inspection of Eq. (4.16b) and using Eqs. (4.12) and (5.1) one has, for $d=4-\varepsilon$,

$$g_{O,O}(x)=[\zeta(d-2,x)+\zeta(d-2,1-x)-2\zeta(d-2)]\times\left[\frac{\pi}{\sin\pi x}\right]^{2-1/\nu}-\varepsilon\frac{N+2}{N+8}\frac{\pi^2}{6}+O(\varepsilon^2)\ , \tag{5.2}$$

which already fulfills the requirement imposed by Eq. (4.23a). Note that $\zeta(d-2,x)+\zeta(d-2,1-x)-2\zeta(d-2)$ remains finite in the limit $d\to 3$ [32] (see below). However, expanding Eq. (5.2) for $x\ll 1$ one obtains

$$g_{O,O}(x)=x^{-(d-1/\nu)}\left[1+\left[2-\frac{1}{\nu}\right]\frac{\pi^2}{6}x^2+(d-2)(d-1)\zeta(d)x^d+O(x^4)\right]-\varepsilon\frac{N+2}{N+8}\frac{\pi^2}{6}+O(\varepsilon^2)\ , \tag{5.3}$$

which is obviously at variance with Eq. (1.3). In order to compensate for the additional x^2 contribution to the short-distance behavior of $g_{O,O}(x)$ shown in Eq. (5.3) we employ the replacement

$$\varepsilon\frac{N+2}{N+8}\frac{\pi^2}{6}\to\left[2-\frac{1}{\nu}\right]\frac{\pi^2}{6}\left[\frac{\pi}{\sin\pi x}\right]^{d-2-1/\nu}, \tag{5.4}$$

which is exact to order ε within the ε expansion, because $d-2-1/\nu=O(\varepsilon)$. The expansion of Eq. (5.4) for $x\ll 1$ yields

$$\left[2-\frac{1}{\nu}\right]\frac{\pi^2}{6}\left[\frac{\pi}{\sin\pi x}\right]^{d-2-1/\nu}=x^{-(d-1/\nu)}\left[2-\frac{1}{\nu}\right]\frac{\pi^2}{6}[x^2+O(x^4)] \tag{5.5}$$

and therefore the short-distance behavior of $g_{O,O}(x)$ takes the corrected form

$$g_{\mathcal{O},\mathcal{O}}(x)=x^{-(d-1/\nu)}[1+(d-2)(d-1)\zeta(d)x^d+O(x^4)] \quad (5.6)$$

if the replacement given by Eq. (5.4) is applied to Eq. (5.2). The exponentiated scaling function $g_{\mathcal{O},\mathcal{O}}(x)$ then reads

$$g_{\mathcal{O},\mathcal{O}}(x)=[\zeta(d-2,x)+\zeta(d-2,1-x)-2\zeta(d-2)]\times\left[\frac{\pi}{\sin\pi x}\right]^{2-1/\nu}-\left[2-\frac{1}{\nu}\right]\frac{\pi^2}{6}\left[\frac{\pi}{\sin\pi x}\right]^{d-2-1/\nu} . \quad (5.7)$$

In $d=3$ Eq. (5.7) can be written as [32]

$$g_{\mathcal{O},\mathcal{O}}(x)=-[\psi(x)+\psi(1-x)+2C]\left[\frac{\pi}{\sin\pi x}\right]^{2-1/\nu}-\left[2-\frac{1}{\nu}\right]\frac{\pi^2}{6}\left[\frac{\pi}{\sin\pi x}\right]^{1-1/\nu} , \quad (5.8)$$

where $\psi(x)=\Gamma'(x)/\Gamma(x)$ denotes the digamma function and $C=-\psi(1)=0.577\,215\,66\ldots$ is Euler's constant.

However, Eq. (5.7) does not represent the only exponentiation of $g_{\mathcal{O},\mathcal{O}}(x)$ which meets the above requirements concerning the short-distance behavior. Returning to Eq. (4.16b) and noting that [32]

$$1+\varepsilon\frac{N+2}{N+8}\ln\frac{\pi}{\sin\pi x}=\zeta(0,x)+\zeta(0,1-x)-2\zeta(0)+\varepsilon\frac{N+2}{N+8}[\zeta'(0,x)+\zeta'(0,1-x)-2\zeta'(0)]$$
$$=\zeta\left[2-\frac{1}{\nu},x\right]+\zeta\left[2-\frac{1}{\nu},1-x\right]-2\zeta\left[2-\frac{1}{\nu}\right]+O(\varepsilon^2) , \quad (5.9)$$

we find the alternative exponentiated form [see Eq. (5.2)]

$$g^{(1)}_{\mathcal{O},\mathcal{O}}(x)=[\zeta(d-2,x)+\zeta(d-2,1-x)-2\zeta(d-2)]\times\left[\zeta\left[2-\frac{1}{\nu},x\right]+\zeta\left[2-\frac{1}{\nu},1-x\right]-2\zeta\left[2-\frac{1}{\nu}\right]\right]-\varepsilon\frac{N+2}{N+8}\frac{\pi^2}{6}+O(\varepsilon^2) . \quad (5.10)$$

The expansion of Eq. (5.10) for $x \ll 1$ yields the short-distance behavior

$$g^{(1)}_{\mathcal{O},\mathcal{O}}(x)=x^{-(d-1/\nu)}\left[1+\left[2-\frac{1}{\nu}\right]\left[3-\frac{1}{\nu}\right]\zeta\left[4-\frac{1}{\nu}\right]x^{4-1/\nu}+(d-2)(d-1)\zeta(d)x^d+O(x^{6-1/\nu})\right]$$
$$-\varepsilon\frac{N+2}{N+8}\frac{\pi^2}{6}+O(\varepsilon^2) , \quad (5.11)$$

which again disagrees with Eq. (1.3). However, in this case the substitution

$$\varepsilon\frac{N+2}{N+8}\frac{\pi^2}{6}\to\left[2-\frac{1}{\nu}\right]\left[3-\frac{1}{\nu}\right]\zeta\left[4-\frac{1}{\nu}\right][\zeta(d-4,x)+\zeta(d-4,1-x)-2\zeta(d-4)] , \quad (5.12)$$

which is exact to order ε, recasts Eq. (5.11) into the form [see Eq. (5.6)]

$$g^{(1)}_{\mathcal{O},\mathcal{O}}(x)=x^{-(d-1/\nu)}[1+(d-2)(d-1)\zeta(d)x^d+O(x^{d+2-1/\nu})] \quad (5.13)$$

so that the exponentiation

$$g^{(1)}_{\mathcal{O},\mathcal{O}}(x)=[\zeta(d-2,x)+\zeta(d-2,1-x)-2\zeta(d-2)]\left[\zeta\left[2-\frac{1}{\nu},x\right]+\zeta\left[2-\frac{1}{\nu},1-x\right]-2\zeta\left[2-\frac{1}{\nu}\right]\right]$$
$$-\left[2-\frac{1}{\nu}\right]\left[3-\frac{1}{\nu}\right]\zeta\left[4-\frac{1}{\nu}\right][\zeta(d-4,x)+\zeta(d-4,1-x)-2\zeta(d-4)] \quad (5.14)$$

yields an alternative for Eq. (5.7). In $d=3$ Eq. (5.14) takes the special form [see Eq. (5.8)]

$$g^{(1)}_{\mathcal{O},\mathcal{O}}(x)=-[\psi(x)+\psi(1-x)+2C]\left[\zeta\left[2-\frac{1}{\nu},x\right]+\zeta\left[2-\frac{1}{\nu},1-x\right]-2\zeta\left[2-\frac{1}{\nu}\right]\right]$$
$$-\left[2-\frac{1}{\nu}\right]\left[3-\frac{1}{\nu}\right]\zeta\left[4-\frac{1}{\nu}\right]x(1-x) , \quad (5.15)$$

where the identity $\zeta(-1,x)=\frac{1}{2}x(1-x)-\frac{1}{12}$ [32] has been used.

There are still other possible exponentiations that are in accordance with our requirements. For brevity we quote only [19]

$$g^{(2)}_{O,O}(x)=[\zeta(d-2,x)+\zeta(d-2,1-x)-2\zeta(d-2)]\times\left[\left[\frac{\pi}{\sin\pi x}\right]^{2-1/\nu}-\frac{(2-1/\nu)\zeta(2)}{\zeta(1/\nu,x)+\zeta(1/\nu,1-x)-2\zeta(1/\nu)}\right] \tag{5.16}$$

and

$$g^{(3)}_{O,O}(x)=[\zeta(d-2,x)+\zeta(d-2,1-x)-2\zeta(d-2)]\times\left[\zeta\left[2-\frac{1}{\nu},x\right]+\zeta\left[\frac{1}{\nu},1-x\right]-2\zeta\left[2-\frac{1}{\nu}\right]-\frac{\left[2-\frac{1}{\nu}\right]\left[3-\frac{1}{\nu}\right]\zeta\left[4-\frac{1}{\nu}\right]}{\zeta(2,x)+\zeta(2,1-x)-2\zeta(2)}\right], \tag{5.17}$$

which can be regarded as modifications of Eqs. (5.7) and (5.14), respectively. Despite the differences in the analytic form of the four exponentiations of $g_{O,O}(x)$ given by Eqs. (5.7), (5.14), (5.16), and (5.17), the numerical differences between them are quite small. The different exponentiations all agree in their short-distance behavior including the leading distant wall correction [see Eqs. (1.3), (5.6), and (5.13)] and therefore the largest deviations between $g_{O,O}(x)$, $g^{(1)}_{O,O}(x)$, $g^{(2)}_{O,O}(x)$, and $g^{(3)}_{O,O}(x)$ can be expected to occur at $x=\frac{1}{2}$. To give an impression of the mutual deviations we quote the following numerical values of the exponentiated scaling function $g_{O,O}(x)$ according to Eqs. (5.7), (5.14), (5.16), and (5.17), respectively, in $d=3$ and for $N=1$:

$$g_{O,O}(\tfrac{1}{2})=4.10,\quad g^{(1)}_{O,O}(\tfrac{1}{2})=4.14\,,\qquad g^{(2)}_{O,O}(\tfrac{1}{2})=4.04,\quad g^{(3)}_{O,O}(\tfrac{1}{2})=4.00\,, \tag{5.18}$$

where $\nu=0.63$ has been used for the correlation length exponent in the Ising universality class [33]. The values shown in Eq. (5.18) should be compared to $g_{O,O}(\frac{1}{2})=3.17$ from the extrapolated ε expansion given by Eqs. (4.16b)–(4.21). According to Eq. (5.18) the relative mutual deviation between $g_{O,O}(x)$, $g^{(1)}_{O,O}(x)$, $g^{(2)}_{O,O}(x)$, and $g^{(3)}_{O,O}(x)$ is at most 3.5% so that the above exponentiations are all equally well suited for our purposes. In the following for numerical convenience we choose $g_{O,O}(x)$ according to Eq. (5.7).

Second, we turn to the scaling function $g_{O,SB}(x)$ [see Eq. (4.18b)], which displays the same form of the short-distance behavior as $g_{O,O}(x)$. Following the line of argument that leads to Eq. (5.7) one arrives at the exponentiated form

$$g_{O,SB}(x)=[\eta(d-2,x)-\eta(d-2,1-x)]\left[\frac{\pi}{\sin\pi x}\right]^{2-1/\nu}+2\eta(d-2)\left[\frac{\pi}{2}\cot\frac{\pi}{2}x\right]^{2-1/\nu}-\frac{2\nu-1}{d\nu-1}\left[\frac{\pi}{\sin\pi x}\right]^{d-1/\nu}, \tag{5.19}$$

where in analogy with Eq. (5.4) the replacement

$$\frac{\varepsilon}{2}\frac{N+2}{N+8}\frac{\pi^2}{\sin^2\pi x}\to\frac{2\nu-1}{d\nu-1}\left[\frac{\pi}{\sin\pi x}\right]^{d-1/\nu} \tag{5.20}$$

has been employed in order to obtain the correct form of the short-distance behavior [see Eqs. (1.3) and (5.6)]. In fact, one obtains from Eq. (5.19) for $x\ll 1$

$$g_{O,SB}(x)=x^{-(d-1/\nu)}\left\{1-\frac{2\nu-1}{d\nu-1}-\left[(d-2)(d-1)\eta(d)+\left[2-\frac{1}{\nu}\right]\frac{\pi^2}{2}\eta(d-2)\right]\times x^d+\cdots\right\}, \tag{5.21}$$

which leads to the exponentiated amplitude relation

$$A_{O,SB}\left[1-\frac{2\nu-1}{d\nu-1}\right]=A_{O,O} \tag{5.22}$$

[see Eqs. (4.16a) and (4.18a)]. Again, Eq. (5.19) does not provide the only possible exponentiation of $g_{O,SB}(x)$, which is in accordance with the required short-distance behavior [see Eq. (5.21)]. However, due to the small numerical deviations of other exponentiations from the one given above we refrain from discussing any alternatives and in the following we stick to Eq. (5.19).

The scaling function $g_{SB,O}(x)$ is given by $g_{O,SB}(1-x)$ [see Eq. (4.18b)] so that one has from Eq. (5.19)

$$g_{SB,O}(x)=-[\eta(d-2,x)-\eta(d-2,1-x)]\left[\frac{\pi}{\sin\pi x}\right]^{2-1/\nu}+2\eta(d-2)\left[\frac{\pi}{2}\tan\frac{\pi}{2}x\right]^{2-1/\nu}-\frac{2\nu-1}{d\nu-1}\left[\frac{\pi}{\sin\pi x}\right]^{d-1/\nu}. \tag{5.23}$$

Using Eq. (5.23) in the limit $x\to 0$ the exponentiated amplitude relation

$$-A_{O,SB}\left[1+\frac{2\nu-1}{d\nu-1}\right]=A_{SB,SB} \tag{5.24}$$

can be inferred from Eq. (4.23a). Note that according to Eq. (4.18a) one has $A_{\mathcal{O},SB}=A_{SB,\mathcal{O}}$. In contrast to Eqs. (5.6) and (5.21) the leading distant wall correction to the short-distance behavior of $g_{SB,\mathcal{O}}(x)$ according to Eq. (5.23) is not governed by x^d. It has been shown in Refs. [19,20] that the leading distant wall correction in this case is governed by an exponent *smaller* than d (see Sec. VI).

Finally, we turn to the scaling function $g_{SB,SB}(x)$. According to Eq. (4.17b), $g_{SB,SB}(x)$ differs from $g_{\mathcal{O},\mathcal{O}}(x)$ only by an additive constant. One option for an exponentiation therefore is to adopt Eq. (5.7) for $g_{\mathcal{O},\mathcal{O}}(x)$ and to extrapolate the additive constant to $\varepsilon=1$. This procedure may look somewhat unsatisfactory. However, naive exponentiations of $g_{SB,SB}(x)$ lead to contributions such as $\zeta(d-2)$, which *diverge* in the limit $d\to 3$. Due to the lack of information on the temperature dependence of the energy density profiles, the additive renormalization scheme given by Eq. (3.11) cannot be applied and therefore these divergences cannot be removed. We thus keep the simple exponentiation scheme for $g_{SB,SB}(x)$ indicated above. In summary, we use the following exponentiated scaling functions:

$$g_{\mathcal{O},\mathcal{O}}(x)=[\zeta(d-2,x)+\zeta(d-2,1-x)-2\zeta(d-2)] \times\left[\frac{\pi}{\sin\pi x}\right]^{2-1/\nu} -\left[2-\frac{1}{\nu}\right]\frac{\pi^2}{6}\left[\frac{\pi}{\sin\pi x}\right]^{d-2-1/\nu}, \tag{5.25a}$$

$$g_{\mathcal{O},SB}(x)=[\eta(d-2,x)-\eta(d-2,1-x)]\left[\frac{\pi}{\sin\pi x}\right]^{2-1/\nu} +2\eta(d-2)\left[\frac{\pi}{2}\cot\frac{\pi}{2}x\right]^{2-1/\nu} -\frac{2\nu-1}{d\nu-1}\left[\frac{\pi}{\sin\pi x}\right]^{d-1/\nu}, \tag{5.25b}$$

and

$$g_{SB,SB}(x)=g_{\mathcal{O},\mathcal{O}}(x)+4\zeta(2)\left\{1-(4-d)\left[\frac{\zeta'(2)}{\zeta(2)}+\frac{N+2}{N+8}(3-\ln 2\pi)\right]\right\} \tag{5.25c}$$

[see Eqs. (4.16b)–(4.21), (5.7), and (5.19)]. For the amplitudes $A_{a,b}$ [see Eqs. (4.16a)–(4.18a)] the naive exponentiation

$$\Gamma\left[\frac{d}{2}-1\right]\left[1-\varepsilon\frac{N+2}{N+8}C\right] =1-C\varepsilon\left[\frac{N+2}{N+8}-\frac{1}{2}\right]+O(\varepsilon^2) =\Gamma\left[\frac{d}{2}+1-\frac{1}{\nu}\right]+O(\varepsilon^2)$$

and Eqs. (5.22) and (5.24) yield

$$A_{\mathcal{O},\mathcal{O}}=\frac{N}{2}\frac{\Gamma\left[\frac{d}{2}+1-\frac{1}{\nu}\right]}{2^d\pi^{d/2}}, \tag{5.26a}$$

$$A_{\mathcal{O},SB}=\frac{d\nu-1}{(d-2)\nu}A_{\mathcal{O},\mathcal{O}}=A_{SB,\mathcal{O}}, \tag{5.26b}$$

and

$$A_{SB,SB}=-\frac{(d+2)\nu-2}{(d-2)\nu}A_{\mathcal{O},\mathcal{O}}. \tag{5.26c}$$

Note that the prefactor $N2^{-d-1}\pi^{-d/2}$ in Eqs. (4.16a)–(4.20) appears in any order of the perturbation theory [see also Eq. (3.4)] and can therefore be taken as an *exact* prefactor of the energy density profile. Numerical values for the amplitudes $A_{\mathcal{O},\mathcal{O}}$, $A_{\mathcal{O},SB}$, and $A_{SB,SB}$ according to Eqs. (5.26a)–(5.26c) are displayed in Table I for $N=1$ and $d=2$, 3, and 4.

In order to demonstrate the effect of the boundary conditions on the shape of the energy density profile $e_{a,b}(0,z,L)$ for $(a,b)=(\mathcal{O},\mathcal{O})$, $(\mathcal{O},SB)$, and (SB,SB) we evaluate Eqs. (5.25a)–(5.26b) numerically for the Ising universality class ($N=1$) in $d=3$. The functional form of $g_{\mathcal{O},\mathcal{O}}(x)$ and $g_{SB,SB}(x)$ in $d=3$ can also be read off from Eq. (5.8). Regarding $g_{\mathcal{O},SB}(x)$ in $d=3$ we note that $\eta(1,x)$ can be represented by the digamma function $\psi(x)$ according to

$$\eta(1,x)=\psi(x)-\psi(x/2)-\ln 2 \tag{5.27}$$

and that in particular

$$\psi(x)-\psi(1-x)=-\pi\cot\pi x \tag{5.28}$$

(see Ref. [32]). The scaling functions of the energy density profiles $e_{\mathcal{O},\mathcal{O}}(0,z,L)$, $e_{\mathcal{O},SB}(0,z,L)$, and $e_{SB,SB}(0,z,L)$ are displayed in Fig. 3, where for $e_{\mathcal{O},SB}(0,z,L)$ the $\mathcal{O}$ wall is located at $z=0$. It is striking that $A_{\mathcal{O},\mathcal{O}}g_{\mathcal{O},\mathcal{O}}(x)$ and

TABLE I. Amplitudes $A_{\mathcal{O},\mathcal{O}}$, $A_{\mathcal{O},SB}$, and $A_{SB,SB}$ according to Eqs. (5.26a)–(5.26c) for $N=1$ and $d=2$, 3, and 4.

d	$A_{\mathcal{O},\mathcal{O}}$	$A_{\mathcal{O},SB}$	$A_{SB,SB}$
2	0.040		
3	0.012	0.017	−0.022
4	0.0032	0.0032	−0.0032

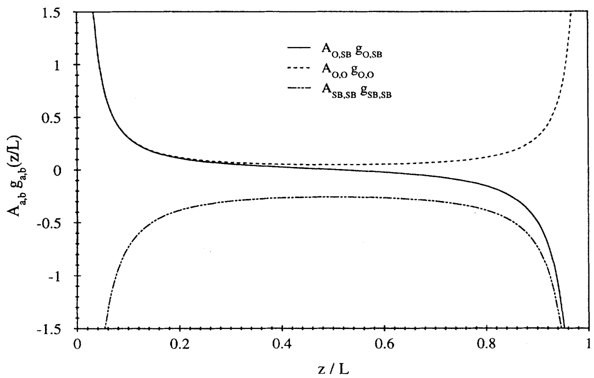

FIG. 3. Scaling functions $A_{\mathcal{O},\mathcal{O}}g_{\mathcal{O},\mathcal{O}}(z/L)$ (dashed line), $A_{\mathcal{O},SB}g_{\mathcal{O},SB}(z/L)$ (solid line; the $\mathcal{O}$ wall is on the left-hand side), and $A_{SB,SB}g_{SB,SB}(z/L)$ (dash-dotted line) in $d=3$ and for $N=1$. The amplitudes $A_{a,b}$ and the scaling functions $g_{a,b}(z/L)$ are taken from Eqs. (5.26) and (5.25), respectively.

$A_{\mathcal{O},SB}g_{\mathcal{O},SB}(x)$ almost coincide up to distances in the order of 25% of the film thickness from the $\mathcal{O}$ wall, whereas $A_{\mathcal{O},SB}g_{\mathcal{O},SB}(x)$ and $A_{SB,SB}g_{SB,SB}(x)$ are clearly distinct even in the vicinity of the SB wall ($x=1$). Close to the walls this behavior can be explained by the difference in the leading distant wall correction to the corresponding semi-infinite energy density profile [see Eq. (4.24)]. Near an $\mathcal{O}$ wall the leading correction to $e_{\mathcal{O},\infty/2}(0,z)$ is governed by $B_{a,b}(z/L)^d$ [see Refs. [19,20], Sec. VI, and Eqs. (5.6) and (5.21)], where the coefficient $B_{a,b}$ depends on the combination (a,b) of the surface universality classes. However, for $z/L \le 0.25$, $(z/L)^d$ with $d=3$ in our case strongly suppresses the difference between $B_{\mathcal{O},\mathcal{O}}$ and $B_{\mathcal{O},SB}$ so that the deviation between $e_{\mathcal{O},\mathcal{O}}(0,z,L)$ and $e_{\mathcal{O},SB}(0,z,L)$ only becomes visible sufficiently far from the $\mathcal{O}$ wall ($z=0$). Near an SB wall the leading distant wall correction is governed by an exponent approximately equal to 1.5 in three dimensions (see Refs. [19,20] and Sec. VI). Therefore the distant wall correction itself is substantially larger near an SB wall than near an $\mathcal{O}$ wall and the deviation between $e_{\mathcal{O},SB}(0,z,L)$ and $e_{SB,SB}(0,z,L)$ for $z<L$ becomes visible even much closer to the SB wall ($z=L$). This means that an $\mathcal{O}$ wall is far more robust against distant wall perturbations than an SB wall. According to Fig. 3 this robustness of the $\mathcal{O}$ wall remains visible as a small deviation between $e_{\mathcal{O},\mathcal{O}}(0,z,L)$ and $e_{\mathcal{O},SB}(0,z,L)$ up to distances z well inside the film.

In two dimensions the surface-bulk (SB) multicritical point does not exist for $N\ge 1$ so that we are restricted to $(a,b)=(\mathcal{O},\mathcal{O})$ for a direct comparison of the energy density profiles in $d=2$, 3, and 4. According to Eq. (1.5) the energy density profile $e_{\mathcal{O},\mathcal{O}}(0,z,L)$ in a two-dimensional strip reads, for the Ising universality class,

$$e_{\mathcal{O},\mathcal{O}}(0,z,L)=A_eL^{-1}\frac{\pi}{\sin\pi x}\ , \tag{5.29}$$

where $x=z/L$. In order to identify the scaling function $g_{\mathcal{O},\mathcal{O}}(x)$ in $d=2$ we note that

$$e_{a,a}(0,z,L)=e_{a,\infty/2}(0,L)g_{a,a}(x)\ , \tag{5.30}$$

which follows from Eqs. (4.11), (4.14), and (4.15). By decomposing the energy density profile given by Eq. (5.29) according to Eq. (5.30) we find

$$g_{\mathcal{O},\mathcal{O}}(x)=\frac{\pi}{\sin\pi x} \tag{5.31}$$

for the Ising universality class in two dimensions. The scaling function $g_{\mathcal{O},\mathcal{O}}(x)$ in $d=3$ and for $N=1$ ($\nu=0.63$) is taken from Eq. (5.7) and in $d=4$ $g_{\mathcal{O},\mathcal{O}}(x)$ can be read off from Eq. (4.16b) for $\varepsilon=0$ [see also Eq. (5.25a) for $\nu=\frac{1}{2}$]. The numerical evaluation of $g_{\mathcal{O},\mathcal{O}}(x)$ in $d=2$, 3, and 4 is displayed in Fig. 4, which shows that the exponentiated scaling function in $d=3$ does not intersect the exact scaling functions in $d=2$ and 4. For fixed scaling argument x $g_{\mathcal{O},\mathcal{O}}(x)$ appears to be a monotonically increasing function of the spatial dimension d. The evaluation of the ε expansion of $g_{\mathcal{O},\mathcal{O}}(x)$ [see Eq. (4.16b)] in the vicinity of $x=\frac{1}{2}$ leads to the same conclusion.

For mixed boundary conditions the scaling functions $g_{a,b}(x)$ in different dimensions in general have an intersection. An example is shown in Fig. 5, where $g_{\mathcal{O},SB}(x)$ is shown in $d=3$ [see Eq. (5.25b)] and in $d=4$ [see Eq. (4.16b) for $\varepsilon=0$] for the Ising universality class. The scaling function $g_{\mathcal{O},SB}(x)$ changes its sign in the interior of the film. The curves intersect, because near the walls $|g_{\mathcal{O},SB}(x\to 0)|$ grows faster in four dimensions than in three dimensions. Note that $e_{\mathcal{O},SB}$ in $d=3,4$ is not antisymmetric around $z=L/2$ in contrast to $e_{+,\mathcal{O}}$ in $d=2$ [see Eq. (1.8)].

It is instructive to evaluate the exponentiated scaling function $g_{\mathcal{O},\mathcal{O}}(x)$ [see Eq. (5.25a)] for $N=1$ in $d=2$, where the exact result is known [see Eq. (5.31)]. From Eq. (5.25a) we obtain in $d=2$ ($\nu=1$)

$$g_{\mathcal{O},\mathcal{O}}(x)=\frac{\pi}{\sin\pi x}\left[1-\frac{1}{6}\sin^2\pi x\right]\ . \tag{5.32}$$

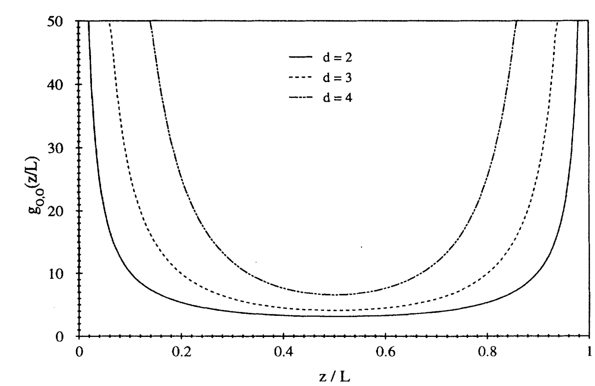

FIG. 4. Scaling functions $g_{\mathcal{O},\mathcal{O}}(z/L)=e_{\mathcal{O},\mathcal{O}}(0,z,L)/e_{\mathcal{O},\infty/2}(0,L)$ in $d=2$ (solid line), $d=3$ (dashed line), and $d=4$ (dash-dotted line) for $N=1$. Numerical evaluations of Eq. (5.31) ($d=2$) and Eq. (5.25a) for $N=1$ in $d=3$ ($\nu=0.63$) and $d=4$ are displayed, respectively.

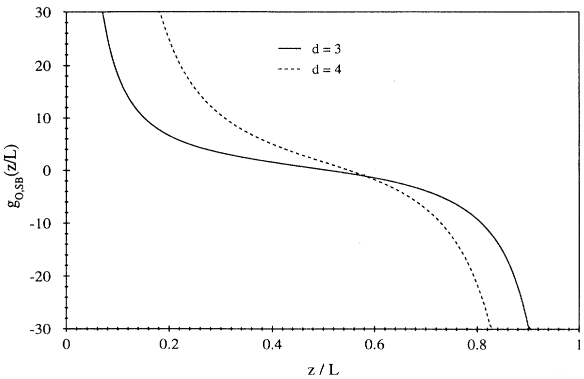

FIG. 5. Scaling functions $g_{\mathcal{O},SB}(z/L)$ in $d=3$ (solid line) and $d=4$ (dashed line) for $N=1$. Numerical evaluations of Eq. (5.25b) for $N=1$ in $d=3$ ($\nu=0.63$) and $d=4$ are displayed, respectively.

As an alternative we also consider Eq. (5.14) from which the result

$$g^{(1)}_{\mathcal{O},\mathcal{O}}(x)=-\psi(x)-\psi(1-x)-2C \qquad (5.33)$$

is obtained, where the identity $\zeta(-2,x)=-\frac{1}{6}x(x-1)(2x-1)$ [32] has been used. For direct comparison $g_{\mathcal{O},\mathcal{O}}(x)$, according to Eqs. (5.32) and (5.33) together with the exact result given by Eq. (5.31), is shown in Fig. 6. The values for $g_{\mathcal{O},\mathcal{O}}(x)$ predicted by Eqs. (5.32) and (5.33) are systematically too small. However, from the numerical point of view the exact shape of $g_{\mathcal{O},\mathcal{O}}(x)$ is reasonably well approximated, whereby Eq. (5.33) yields slightly better results than Eq. (5.32). The other two exponentiations according to Eqs. (5.16) and (5.17), which are not shown in Fig. 6, yield approximations in the same range of precision as provided by Eqs. (5.32) and (5.33). However, in $d=2$ the exponentiations according to Eqs. (5.7), (5.14), (5.16), and (5.17) suffer from the deficiency that they do not reproduce the correct leading distant wall correction, which is given by the x^2 term in the expansion

$$g_{\mathcal{O},\mathcal{O}}(x)=\frac{\pi}{\sin\pi x}=\frac{1}{x}\left[1+\frac{\pi^2}{6}x^2+\cdots\right]. \qquad (5.34)$$

Instead, leading distant wall corrections of the order x^3 or higher are obtained from the exponentiations. In order to investigate this deficiency systematically we now compare the short-distance behavior of the exponentiated energy density profiles with results from the ε expansion.

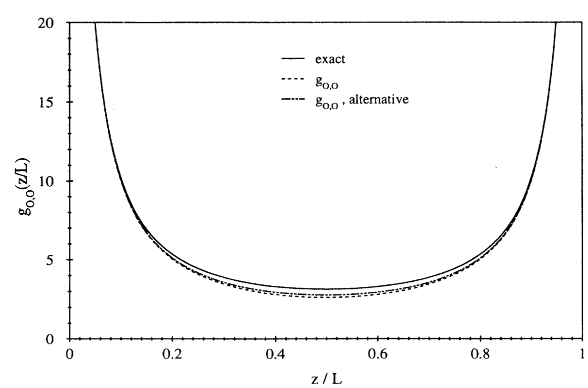

FIG. 6. Scaling function $g_{\mathcal{O},\mathcal{O}}(z/L)$ in $d=2$ and for $N=1$ according to Eq. (5.31) (solid line), Eq. (5.32) (dashed line), and Eq. (5.33) (dash-dotted line). The solid line shows the exact result, whereas the dashed and the dash-dotted lines show evaluations of different exponentiations for the scaling function $g_{\mathcal{O},\mathcal{O}}(z/L)$ in $d=2$ and for $N=1$.

VI. SHORT-DISTANCE BEHAVIOR OF THE ENERGY DENSITY PROFILES

For the exponentiation of the energy density profiles in Sec. V, some information about the structure of the short-distance behavior of the scaling functions has been used in an exponentiated form. However, the ε expansion of the energy density profiles given by Eqs. (4.6)–(4.10) or, equivalently, the ε expansion of the scaling functions $g_{a,b}(x)$ given by Eqs. (4.16b)–(4.21) does not necessarily contain enough information to identify the *exponents* of the distant wall corrections to the required order in ε. To illustrate this we consider the following example. Let $g(x)$ be a universal scaling function that has the short-distance behavior

$$g(x)=ax^{\alpha}+bx^{\beta}+\cdots. \qquad (6.1)$$

With the ε expansion of the amplitudes $a=a_0+\varepsilon a_1+O(\varepsilon^2)$ and $b=b_0+\varepsilon b_1+O(\varepsilon^2)$ and the exponents $\alpha=\alpha_0+\varepsilon\alpha_1+O(\varepsilon^2)$ and $\beta=\beta_0+\varepsilon\beta_1+O(\varepsilon^2)$, we have to first order in ε

$$g(x)=x^{\alpha_0}[a_0+\varepsilon(a_1+a_0\alpha_1\ln x)+O(\varepsilon^2)] + x^{\beta_0}[b_0+\varepsilon(b_1+b_0\beta_1\ln x)+O(\varepsilon^2)]+\cdots. \qquad (6.2)$$

If $\alpha_0\neq\beta_0$ the coefficients a_0 and b_0 can be identified from Eq. (6.2) by inspection and, knowing a_0 and b_0, the logarithmic terms yield α_1 and β_1 so that Eq. (6.1) can indeed be reconstructed from Eq. (6.2), where amplitudes and exponents are known to order ε. However, if $\alpha_0=\beta_0$ this is no longer possible. As a_0 and b_0 cannot be identified from Eq. (6.2), in this case α_1 and β_1 remain unknown as well.

In order to obtain the correct short-distance behavior of the energy density profiles to first order in ε from the ε expansion given by Eqs. (4.6)–(4.10) additional information about the exponents of the distant wall corrections is needed. This additional information can be obtained from the *short-distance expansion* of the energy density scaling operator near the wall in a semi-infinite geometry [19,20]. The exponents in question are given by the scaling dimensions of the *surface operators,* which govern the short-distance expansion of the energy density. Near an $\mathcal{O}$ wall the leading distant wall correction is governed by the exponent $d=4-\varepsilon$ [18–20] so that the structure of the short-distance behavior anticipated by Eq. (1.3) [12] is indeed correct. Near an SB wall the leading distant wall correction is governed by the exponent $d-1-\Phi/\nu<d$ [19,20], where

$$\Phi=\frac{1}{2}-\frac{\varepsilon}{4}\frac{N+2}{N+8}+O(\varepsilon^2) \tag{6.3}$$

is the so-called crossover exponent [5]. The next-to-leading distant wall corrections are governed by exponents that differ from the leading ones d and $d-1-\Phi/\nu$, respectively, by an amount of order ε^0 [19,20].

Using the above exponents the short-distance behavior of the energy density profiles $e_{a,b}(0,z,L)$ can be cast into the form

$$e_{\mathcal{O},b}(0,z,L)=e_{\mathcal{O},\infty/2}(0,z)\left[1+B_{\mathcal{O},b}\left[\frac{z}{L}\right]^d+\cdots\right] \tag{6.4a}$$

and

$$e_{SB,b}(0,z,L)=e_{SB,\infty/2}(0,z)\left[1+A_{SB,b}\left[\frac{z}{L}\right]^{d-1-\Phi/\nu}+\cdots\right], \tag{6.4b}$$

where $b=\mathcal{O},SB$ and $e_{\mathcal{O},\infty/2}(0,z)$ and $e_{SB,\infty/2}(0,z)$ are given by Eq. (4.15). From the ε expansion of the energy density profiles [see Eqs. (4.6)–(4.10)] the coefficients $B_{\mathcal{O},b}$ and $A_{SB,b}$ can now be determined to order ε. One finds

$$B_{\mathcal{O},\mathcal{O}}=6\zeta(4)\left[1-\varepsilon\left[\frac{5}{6}+\frac{\zeta'(4)}{\zeta(4)}-\frac{1}{12}\frac{N+2}{N+8}\right]\right], \tag{6.5a}$$

$$B_{\mathcal{O},SB}=-6\eta(4)\left[1-\varepsilon\left[\frac{5}{6}+\frac{\eta'(4)}{\eta(4)}-\frac{71}{42}\frac{N+2}{N+8}\right]\right], \tag{6.5b}$$

$$A_{SB,\mathcal{O}}=-4\eta(2)\left\{1-\varepsilon\left[\frac{\eta'(2)}{\eta(2)}+\frac{N+2}{N+8}\left[\frac{3}{2}-\ln\frac{\pi}{2}\right]\right]\right\}, \tag{6.5c}$$

and

$$A_{SB,SB}=4\zeta(2)\left[1-\varepsilon\left[\frac{\zeta'(2)}{\zeta(2)}\frac{N+2}{N+8}[3-\ln(2\pi)]\right]\right]. \tag{6.5d}$$

It is a general deficiency of the exponentiated scaling functions $g_{SB,\mathcal{O}}(x)$ and $g_{SB,SB}(x)$ that Eqs. (6.4a) and (6.4b) are reproduced only in the Gaussian approximation ($\Phi=\nu=\frac{1}{2}$) by the corresponding energy density profiles $e_{SB,\mathcal{O}}(0,z,L)$ and $e_{SB,SB}(0,z,L)$ in general dimension d. The exponentiated energy density profile $e_{SB,\mathcal{O}}(0,z,L)$ [see Eq. (5.23) and Eqs. (5.26a)–(5.26c)] yields various distant wall corrections with exponents smaller than d. However, none of these is in accordance with Eqs. (6.4a) and (6.4b). The exponentiation of the energy density profile $e_{SB,SB}(0,z,L)$ yields the exponent $d-1/\nu$ for the leading distant wall correction. In fact, from the ε expansions for ν [see Eq. (4.2)] and Φ [see Eq. (6.3)] one finds $d-1-\Phi/\nu=d-1/\nu+O(\varepsilon^2)$, so that the misrepresentation of the leading distant wall correction by $g_{SB,SB}(x)$ in Eq. (5.25c) may be an artifact of the truncation of the ε expansion of Eqs. (4.6)–(4.10) and in Eqs. (4.16b)–(4.21) after contributions of first order in ε. The exponentiated scaling functions $g_{\mathcal{O},\mathcal{O}}(x)$ and $g_{\mathcal{O},SB}(x)$ reproduce Eqs. (6.4a) and (6.4b) by construction, but the coefficients $B_{\mathcal{O},\mathcal{O}}$ and $B_{\mathcal{O},SB}$ in the exponentiated form do not correctly incorporate the two-loop contribution shown in Eqs. (6.5a)–(6.5d) [see Eqs. (5.6) and (5.21), respectively]. The exponentiation scheme described in Sec. V therefore only yields the global shape of the profiles in an apparently reliable form (see Fig. 6). However, local information such as the short-distance expansion is not properly represented by the exponentiations discussed here. In order to obtain this piece of information one has to resort to the explicit short-distance expansion of the energy density scaling operator within the field-theoretic renormalization group [19,20].

VII. SUMMARY AND CONCLUSIONS

As a paradigm for scaling density profiles in critical films in d dimensions we have studied the energy density profiles of an O(N)-symmetric critical system for symmetry-conserving boundary conditions by field-theoretic methods. The following main results have been obtained.

(i) By solving the renormalization-group equations for the renormalized energy density profile it has been shown that the singular part of the energy density profile is governed by a scaling function that is universal up to a nonuniversal amplitude factor. The amplitude factor can be expressed by the nonuniversal bulk correlation length amplitude, which allows one to identify the universal scaling function from a field-theoretic calculation. If the scaling function is determined this way, it depends on the definition adopted for the bulk correlation length.

(ii) The energy density profiles and the corresponding scaling functions have been calculated to two-loop order at bulk criticality for symmetry-conserving boundary conditions, i.e., for any combination of the $\mathcal{O}$- and the SB-surface universality classes at the surfaces of the film and for periodic and antiperiodic boundary conditions, where the profile is constant in the latter two cases.

(iii) Using the ε expansion of the scaling functions and some information about the short-distance behavior of the energy density profiles simple exponentiations of the scaling functions can be found. The exponentiation is not unique, but different exponentiation schemes lead to almost identical numerical results. In $d=3$ a direct comparison of the energy density profiles in critical films for $(a,b)=(\mathcal{O},\mathcal{O})$, $(\mathcal{O},SB)$, and (SB,SB) shows that an $\mathcal{O}$ wall is much more robust against perturbations from the second (far) wall than the SB wall. For small distances from the wall the same conclusions can be drawn from a short-distance expansion of the energy density scaling operator. In $d=2$ and for $(a,b)=(\mathcal{O},\mathcal{O})$, where an exact result for the energy density profile is available, the exponentiation scheme used here leads to a reasonable agreement with the exact profile shape. Due to the absence of the *SB* multicritical point in $d=2$ and for $N \geq 1$ an extension of our considerations to the order parameter or the energy density profile in the presence of surface fields, i.e., symmetry-breaking boundary conditions, is desirable in order to cover a wider range of boundary conditions that are also realized in two dimensions.

(iv) With additional information from the short-distance expansion of the energy density the coefficients of the leading distant wall corrections for the energy density profile near an $\mathcal{O}$ and an *SB* wall can be obtained from the ε expansion of the scaling functions. A comparison of the short-distance behavior of the exponentiated energy density profiles with corresponding results from the ε expansion shows that the exponentiation near an $\mathcal{O}$ wall fails to represent the two-loop contribution to the leading distant wall correction correctly. Near an *SB* wall the exponentiation fails to give the correct exponent of the leading distant wall correction, which is partly due to the truncation of the ε expansion at the order ε. In order to elucidate the structure of the short-distance behavior of scaling density profiles an investigation of the short-distance expansion by field-theoretic methods is required.

ACKNOWLEDGMENT

The research of M. Krech and S. Dietrich has been supported in part by the Deutsche Forschungsgemeinschaft through Sonderforschungsbereich No. 237 "Unordnung and groβe Fluktuationen."

APPENDIX A: INTEGRALS OVER HURWITZ AND BIVARIATE η FUNCTIONS

In the course of the calculation of the energy density profiles several integrals over Hurwitz and bivariate η functions have to be evaluated in dimensional regularization. In the following these integrals will be discussed in some detail.

Both the Hurwitz and the bivariate η function are special cases of Lerch's function $\Phi(p,\alpha,x)$, which can be defined as [32]

$$\Phi(p,\alpha,x)=\sum_{n=0}^{\infty}\frac{p^n}{(n+x)^\alpha} \tag{A1}$$

for $|p|<1$ and $x\neq 0,-1,-2,\ldots$. Usually p, α, and x are denoted as the *argument*, the *order*, and the *parameter* of Lerch's function, respectively. Then the Hurwitz function $\zeta(\alpha,x)$ and the bivariate η function $\eta(\alpha,x)$ have the representation [32]

$$\zeta(\alpha,x)=\Phi(1,\alpha,x),\quad \eta(\alpha,x)=\Phi(-1,\alpha,x) \tag{A2}$$

so that the well-known series representations of $\zeta(\alpha,x)$ for $\mathrm{Re}\alpha>1$ and of $\eta(\alpha,x)$ for $\mathrm{Re}\alpha>0$ can be read off from Eq. (A1). Furthermore, Lerch's function obeys the recursion relation [32]

$$\Phi(p,\alpha,x)=p\Phi(p,\alpha,x+1)+x^{-\alpha}, \tag{A3}$$

which generalizes the recursion relations for $\zeta(\alpha,x)$ and $\eta(\alpha,x)$ accordingly.

The indefinite integral of $\Phi(p,\alpha,x)$ with respect to the parameter x for $\alpha\neq 1$ can be written as

$$\int\Phi(p,\alpha,x)dx=\frac{-1}{\alpha-1}\Phi(p,\alpha-1,x) \tag{A4}$$

and therefore one has for $\mathrm{Re}\alpha<1$

$$\int_0^1\Phi(p,\alpha,x)dx=\frac{p-1}{\alpha-1}\Phi(p,\alpha-1,1), \tag{A5}$$

where the recursion relation in Eq. (A3) has been used for $x=0$. For $p=1$ and -1 the important identities

$$\int_0^1\zeta(\alpha,x)dx=0,\quad \int_0^1\eta(\alpha,x)dx=\frac{2}{1-\alpha}\eta(\alpha-1) \tag{A6}$$

follow provided $\mathrm{Re}\alpha<1$. The calculation of the energy density profiles involves Hurwitz and bivariate η functions with dimension-dependent orders α. For the spatial dimensions d of interest the condition $\mathrm{Re}\alpha<1$, which is necessary for the validity of Eq. (A6), is not satisfied. However, in the spirit of the dimensional regularization scheme the right-hand sides of Eq. (A6) are interpreted as the *analytic continuations* of the corresponding integrals to the region $\mathrm{Re}\alpha>1$. For the integral over the Hurwitz function this is trivial, for the integral over the bivariate η function the analytic continuation is provided by the η function $\eta(\alpha)=\eta(\alpha,1)$ as a function of its order α. The corresponding *dimensionally regularized* integrals required for the calculation of the energy density profiles are therefore given by the right-hand sides of Eq. (A6).

A second type of integral involves products of Hurwitz functions of the form $\zeta(\alpha,x)\zeta(\beta,1-x)$ and products of bivariate η functions of the same form, which therefore can be generalized to the product $\Phi(p,\alpha,x)\Phi(p,\beta,1-x)$ of Lerch's functions. For $\mathrm{Re}\alpha<1$ and $\mathrm{Re}\beta<1$ we consider the integral $\int_0^1\Phi(p,\alpha,x)\Phi(p,\beta,1-x)dx$, which can be evaluated in a straightforward manner if $|p|<1$. Using Eq. (A1) one has

$$\int_0^1 \Phi(p,\alpha,x)\Phi(p,\beta,1-x)dx = \sum_{m,n=1}^{\infty} p^{m+n}\int_0^1 \frac{dx}{(m+x)^\alpha (n+x)^\beta}$$
$$= \sum_{k=0}^{\infty}\sum_{j=0}^{k} p^k \int_0^1 \frac{dx}{(j+x)^\alpha (k-j+1-x)^\beta}$$
$$= \sum_{k=0}^{\infty} p^k \sum_{j=0}^{k}\int_j^{j+1} \frac{dx}{x^\alpha (k+1-x)^\beta}$$
$$= \sum_{k=0}^{\infty} p^k \int_0^{k+1} \frac{dx}{x^\alpha (k+1-x)^\beta}$$
$$= \sum_{k=0}^{\infty} \frac{p^k}{(k+1)^{\alpha+\beta-1}}\int_0^1 \frac{dx}{x^\alpha (1-x)^\beta}$$
$$= \Phi(p,\alpha+\beta-1,1)B(1-\alpha,1-\beta) , \tag{A7}$$

where $B(u,v)$ is Euler's beta function. The analytic continuation of Eq. (A7) to $p=1$ and -1 leads to the important identities

$$\int_0^1 \zeta(\alpha,x)\zeta(\beta,1-x)dx = \zeta(\alpha+\beta-1)B(1-\alpha,1-\beta) \tag{A8a}$$

and

$$\int_0^1 \eta(\alpha,x)\eta(\beta,1-x)dx = \eta(\alpha+\beta-1)B(1-\alpha,1-\beta) , \tag{A8b}$$

which hold rigorously for $\mathrm{Re}\alpha<1$ and $\mathrm{Re}\beta<1$. The energy density profiles involve integrals as shown in Eqs. (A8a) and (A8b) with dimension-dependent orders α and β. Again, the conditions $\mathrm{Re}\alpha<1$ and $\mathrm{Re}\beta<1$ do not hold for the spatial dimensions of interest. However, in the same spirit as in Eq. (A6) the right-hand sides of Eqs. (A8a) and (A8b) provide the dimensionally regularized integrals.

A third type of integral involves products of Hurwitz and bivariate η functions at the same value of the parameter x that has the generalized form $\Phi(p,\alpha,x)\Phi(q,\beta,x)$. The integral $\int_0^1 \Phi(p,a,x)\Phi(q,\beta,x)dx$, which we will discuss below, exists only in the region described by the inequalities $\mathrm{Re}\alpha<1$, $\mathrm{Re}\beta<1$, and $\mathrm{Re}(\alpha+\beta)<1$. For $|p|<1$ and $|q|<1$ Eq. (A1) can be used to obtain the expansion

$$\int_0^1 \Phi(p,\alpha,x)\Phi(q,\beta,x)dx = \sum_{m,n=0}^{\infty} p^m q^n \int_0^1 \frac{dx}{(m+x)^\alpha (n+x)^\beta}$$
$$= \sum_{m=0}^{\infty}\sum_{n=m+1}^{\infty}\left[p^m q^n \int_0^1 \frac{dx}{(m+x)^\alpha (n+x)^\beta} + p^n q^m \int_0^1 \frac{dx}{(n+x)^\alpha (m+x)^\beta}\right]$$
$$+ \sum_{m=0}^{\infty} (pq)^m \int_0^1 \frac{dx}{(m+x)^{\alpha+\beta}}$$
$$= \sum_{m=0}^{\infty}\sum_{k=1}^{\infty} (pq)^m \left[q^k \int_m^{m+1} \frac{dx}{x^\alpha (k+x)^\beta} + p^k \int_m^{m+1} \frac{dx}{x^\beta (k+x)^\alpha}\right] + \frac{pq-1}{\alpha+\beta-1}\Phi(pq,\alpha+\beta-1,1)$$
$$= \sum_{m=0}^{\infty} (pq)^m \left[q\int_m^{m+1} x^{-\alpha}\Phi(q,\beta,x+1)dx + p\int_m^{m+1} x^{-\beta}\Phi(p,\alpha,x+1)dx \right]$$
$$+ \frac{pq-1}{\alpha+\beta-1}\Phi(pq,\alpha+\beta-1,1) , \tag{A9}$$

where Eq. (A5) has been used. By inspection of the right-hand side of Eq. (A9) one finds that the condition $\mathrm{Re}(\alpha+\beta)<1$ is no longer needed so that an analytic continuation of the left-hand side of Eq. (A9) into the region $\{\alpha,\beta|\mathrm{Re}\alpha<1, \mathrm{Re}\beta<1, \mathrm{Re}(\alpha+\beta)>1\}$ has been achieved. For $\mathrm{Re}(\alpha+\beta)>1$ the limit $p\to e^{i\lambda}$, $q\to e^{-i\lambda}$ for real $\lambda\neq 0$ can be performed on the right-hand side of Eq. (A9), which leads to the integral

$$\int_0^\infty [x^{-\alpha}e^{-i\lambda}\Phi(e^{-i\lambda},\beta,x+1)+x^{-\beta}e^{i\lambda}\Phi(e^{i\lambda},\alpha,x+1)]dx .$$

Note that the requirements $\mathrm{Re}\alpha<1$, $\mathrm{Re}\beta<1$, and $\mathrm{Re}(\alpha+\beta)>1$ guarantee the convergence of the above integral for $\lambda\neq 0$. Using Eq. (A1) one finds for these conditions

$$\int_0^\infty [x^{-\alpha}e^{-i\lambda}\Phi(e^{-i\lambda},\beta,x+1)+x^{-\beta}e^{i\lambda}\Phi(e^{i\lambda},\alpha,x+1)]dx$$
$$=e^{-i\lambda}\sum_{n=0}^\infty e^{-in\lambda}\int_0^\infty \frac{dx}{x^\alpha(n+1+x)^\beta}+e^{i\lambda}\sum_{n=0}^\infty e^{in\lambda}\int_0^\infty \frac{dx}{x^\beta(n+1+x)^\alpha}$$
$$=e^{-i\lambda}\sum_{n=0}^\infty \frac{e^{-in\lambda}}{(n+1)^{\alpha+\beta-1}}\int_0^\infty \frac{dx}{x^\alpha(1+x)^\beta}+e^{i\lambda}\sum_{n=0}^\infty \frac{e^{in\lambda}}{(n+1)^{\alpha+\beta-1}}\int_0^\infty \frac{dx}{x^\beta(1+x)^\alpha}$$
$$=e^{-i\lambda}\Phi(e^{-i\lambda},\alpha+\beta-1,1)B(\alpha+\beta-1,1-\alpha)+e^{i\lambda}\Phi(e^{i\lambda},\alpha+\beta-1,1)B(\alpha+\beta-1,1-\beta)\ . \tag{A10}$$

The analytic continuations of Lerch's function and Euler's beta function back to the regime $\mathrm{Re}(\alpha+\beta)<1$ establish the useful relation

$$\int_0^1 \Phi(e^{i\lambda},\alpha,x)\Phi(e^{-i\lambda},\beta,x)dx =e^{-i\lambda}\Phi(e^{-i\lambda},\alpha+\beta-1,1)B(\alpha+\beta-1,1-\alpha) +e^{i\lambda}\Phi(e^{i\lambda},\alpha+\beta-1,1)B(\alpha+\beta-1,1-\beta)\ , \tag{A11}$$

where the right-hand side again provides the analytic continuation of the integral in terms of the orders α and β. Moreover, Eq. (A11) allows one to perform the limit $\lambda\to 0$, which together with the special value $\lambda=\pi$ yields the important identities

$$\int_0^1 \zeta(\alpha,x)\zeta(\beta,x)dx=\zeta(\alpha+\beta-1)[B(\alpha+\beta-1,1-\alpha) +B(\alpha+\beta-1,1-\beta)] \tag{A12a}$$

and

$$\int_0^1 \eta(\alpha,x)\eta(\beta,x)dx =-\eta(\alpha+\beta-1)[B(\alpha+\beta-1,1-\alpha) +B(\alpha+\beta-1,1-\beta)] \tag{A12b}$$

for $\mathrm{Re}\alpha<1$, $\mathrm{Re}\beta<1$, and $\mathrm{Re}(\alpha+\beta)<1$. In the spirit of Eq. (A6) the right-hand sides of Eqs. (A12a) and (A12b) provide the dimensional regularization of the corresponding dimension-dependent integrals in the energy density profiles.

APPENDIX B: PROPAGATORS AND VERTICES

In order to implement the perturbation expansion of the energy density profiles in terms of Feynman graphs the O(N)-symmetric Ginzburg-Landau Hamiltonian in a film geometry [see Eq. (2.1)] that can be decomposed according to $\mathcal{H}=\mathcal{H}_0+\mathcal{H}_I$ is written in spectral representation with respect to the parallel coordinate $\mathbf{r}_\parallel$. The Gaussian part $\mathcal{H}_0$ and the interaction part $\mathcal{H}_I$ of the Hamiltonian $\mathcal{H}$ are given by

$$\mathcal{H}_0[\mathbf{\Phi}]=\frac{1}{2}\int_0^L dz\int d^{d-1}p\left[\left[\frac{\partial}{\partial z}\mathbf{\Phi}(\mathbf{p},z)\right]\cdot\left[\frac{\partial}{\partial z}\mathbf{\Phi}(-\mathbf{p},z)\right]+(\mathbf{p}^2+\tau)\mathbf{\Phi}(\mathbf{p},z)\cdot\mathbf{\Phi}(-\mathbf{p},z)\right] +\frac{1}{2}\int d^{d-1}p[c_a\mathbf{\Phi}(\mathbf{p},0)\cdot\mathbf{\Phi}(-\mathbf{p},0)+c_b\mathbf{\Phi}(\mathbf{p},L)\cdot\mathbf{\Phi}(-\mathbf{p},L)] \tag{B1}$$

and

$$\mathcal{H}_I[\mathbf{\Phi}]=\frac{g}{4!}\frac{1}{(2\pi)^{d-1}}\int_0^L dz\int d^{d-1}p_1\cdots d^{d-1}p_4 \times\delta^{(d-1)}(\mathbf{p}_1+\mathbf{p}_2+\mathbf{p}_3+\mathbf{p}_4) \times(\mathbf{\Phi}(\mathbf{p}_1,z)\cdot\mathbf{\Phi}(\mathbf{p}_2,z)) \times(\mathbf{\Phi}(\mathbf{p}_3,z)\cdot\mathbf{\Phi}(\mathbf{p}_4,z))\ , \tag{B2}$$

respectively, where bulk and surface fields have been disregarded and the order parameter field $\mathbf{\Phi}$ is an N component vector according to $\mathbf{\Phi}(\mathbf{p},z)=(\phi_1(\mathbf{p},z),\ldots,\phi_N(\mathbf{p},z))$. For a complete spectral representation of Eq. (2.1) see Appendix A of Ref. [26]. In the following we focus on Dirichlet (D), Neumann (N), periodic (per), and antiperiodic (aper) boundary conditions as given by Eqs. (2.2) and (2.3). Note that for periodic and antiperiodic boundary conditions the surface contribution to $\mathcal{H}_0$ in Eq. (B1) is absent. The free propagator $G_{ij}^{(0)a,b}(\mathbf{p},\mathbf{p}';z,z')$ for the combination a,b of boundary conditions is defined by the Gaussian average

$$G_{ij}^{(0)a,b}(\mathbf{p},\mathbf{p}';z,z')=\langle\phi_i(\mathbf{p},z)\phi_j(\mathbf{p}',z')\rangle_{\mathcal{H}_0}\ . \tag{B3}$$

According to Eq. (B3) one obtains for $\tau\geq 0$ and $0\leq z, z'\leq L$ in the case of equal boundary conditions

$$G_{ij}^{(0)D,D}(\mathbf{p},\mathbf{p}';z,z')=\frac{\delta_{ij}\delta^{(d-1)}(\mathbf{p}+\mathbf{p}')}{\sqrt{\mathbf{p}^2+\tau}\sinh(\sqrt{\mathbf{p}^2+\tau}L)}\sinh[\tfrac{1}{2}\sqrt{\mathbf{p}^2+\tau}(z+z'-|z-z'|)]\times\sinh[\tfrac{1}{2}\sqrt{\mathbf{p}^2+\tau}(2L-z-z'-|z-z'|)] \quad \text{(B4)}$$

and

$$G_{ij}^{(0)N,N}(\mathbf{p},\mathbf{p}';z,z')=\frac{\delta_{ij}\delta^{(d-1)}(\mathbf{p}+\mathbf{p}')}{\sqrt{\mathbf{p}^2+\tau}\sinh(\sqrt{\mathbf{p}^2+\tau}L)}\cosh[\tfrac{1}{2}\sqrt{\mathbf{p}^2+\tau}(z+z'-|z-z'|)]\times\cosh[\tfrac{1}{2}\sqrt{\mathbf{p}^2+\tau}(2L-z-z'-|z-z'|)]\ . \quad \text{(B5)}$$

The mixed boundary conditions are described by

$$G_{ij}^{(0)D,N}(\mathbf{p},\mathbf{p}';z,z')=\frac{\delta_{ij}\delta^{(d-1)}(\mathbf{p}+\mathbf{p}')}{\sqrt{\mathbf{p}^2+\tau}\cosh(\sqrt{\mathbf{p}^2+\tau}L)}\sinh[\tfrac{1}{2}\sqrt{\mathbf{p}^2+\tau}(z+z'-|z-z'|)]\times\cosh[\tfrac{1}{2}\sqrt{\mathbf{p}^2+\tau}(2L-z-z'-|z-z'|)]\ . \quad \text{(B6)}$$

For periodic and antiperiodic boundary conditions one has

$$G_{ij}^{(0)\mathrm{per}}(\mathbf{p},\mathbf{p}';z,z')=\frac{\delta_{ij}\delta^{(d-1)}(\mathbf{p}+\mathbf{p}')}{2\sqrt{\mathbf{p}^2+\tau}\sinh(\tfrac{1}{2}\sqrt{\mathbf{p}^2+\tau}L)}\times\cosh[\tfrac{1}{2}\sqrt{\mathbf{p}^2+\tau}(L-2|z-z'|)] \quad \text{(B7)}$$

and

$$G_{ij}^{(0)\mathrm{aper}}(\mathbf{p},\mathbf{p}';z,z')=\frac{\delta_{ij}\delta^{(d-1)}(\mathbf{p}+\mathbf{p}')}{2\sqrt{\mathbf{p}^2+\tau}\cosh(\tfrac{1}{2}\sqrt{\mathbf{p}^2+\tau}L)}\times\sinh[\tfrac{1}{2}\sqrt{\mathbf{p}^2+\tau}(L-2|z-z'|)]\ , \quad \text{(B8)}$$

respectively. Note that $G_{ij}^{(0)N,D}(\mathbf{p},\mathbf{p}';z,z')=G_{ij}^{(0)D,N}(\mathbf{p},\mathbf{p}';L-z,L-z')$. The interaction part $\mathcal{H}_I$ of the Ginzburg-Landau Hamiltonian [see Eq. (B2)] can be written in the form

$$\mathcal{H}_I[\Phi]=\int_0^L\int d^{d-1}p_1\cdots d^{d-1}p_4\times\sum_{i,j,k,l}v_{ijkl}(\mathbf{p}_1,\mathbf{p}_2,\mathbf{p}_3,\mathbf{p}_4)\phi_i(\mathbf{p}_1,z)\times\phi_j(\mathbf{p}_2,z)\phi_k(\mathbf{p}_3,z)\phi_l(\mathbf{p}_4,z)\ ,$$

where the vertex function v_{ijkl} is given by (see also Ref. [1])

$$v_{ijkl}(\mathbf{p}_1,\mathbf{p}_2,\mathbf{p}_3,\mathbf{p}_4)=\frac{g}{4!}\frac{1}{(2\pi)^{d-1}}\frac{1}{3}\times(\delta_{ij}\delta_{kl}+\delta_{ik}\delta_{jl}+\delta_{il}\delta_{jk})\times\delta^{(d-1)}(\mathbf{p}_1+\mathbf{p}_2+\mathbf{p}_3+\mathbf{p}_4) \quad \text{(B9)}$$

for all boundary conditions considered here.

APPENDIX C: ENERGY DENSITY PROFILES TO ONE-LOOP ORDER

The one-loop contribution $\bar{e}_{a,b}^{(1)}(\tau,z,L)$ to the bare energy density profile $\bar{e}_{a,b}(\tau,z,L)$ can be represented in the form

$$\bar{e}_{a,b}^{(1)}(\tau,z,L)=-\frac{N}{2}\int\frac{d^{d-1}p}{(2\pi)^{d-1}}G^{(0)a,b}(\mathbf{p};z,z)\ , \quad \text{(C1)}$$

where $G^{(0)a,b}(\mathbf{p};z,z')$ is defined by

$$G_{i,j}^{(0)a,b}(\mathbf{p},\mathbf{p}';z,z')=\delta_{ij}\delta^{(d-1)}(\mathbf{p}+\mathbf{p}')G^{(0)a,b}(\mathbf{p};z,z')\ . \quad \text{(C2)}$$

The Green's functions $G^{(0)a,b}(\mathbf{p};z,z')$ can be read off directly from Eqs. (B4)–(B8) for all boundary conditions under consideration.

At bulk criticality, i.e., for $\tau=0$ the evaluation of $\bar{e}_{a,b}^{(1)}$ according to Eq. (C1) requires the calculation of the integrals

$$\int_0^\infty\frac{y^{\alpha-1}e^{-xy}}{\sinh y}dy,\quad\int_0^\infty\frac{y^{\alpha-1}e^{-xy}}{\cosh y}dy$$

as functions of the variables α and x. For the first integral one obtains for real $\alpha>1$ and $x>-1$

$$\int_0^\infty\frac{y^{\alpha-1}e^{-xy}}{\sinh y}dy=2\int_0^\infty\frac{y^{\alpha-1}e^{-(x+1)y}}{1-e^{-2y}}dy=2\sum_{n=0}^\infty\int_0^\infty y^{\alpha-1}e^{-(x+1+2n)y}dy=2\sum_{n=0}^\infty\frac{1}{(2n+1+x)^\alpha}\int_0^\infty y^{\alpha-1}e^{-y}dy=2^{1-\alpha}\Gamma(\alpha)\zeta\left[\alpha,\frac{x+1}{2}\right]\ , \quad \text{(C3)}$$

where $\Gamma(\alpha)$ denotes the Γ function. Likewise, the second integral yields for $\alpha>0$ and $x>-1$

$$\int_0^\infty \frac{y^{\alpha-1}e^{-xy}}{\cosh y}dy=2^{1-\alpha}\Gamma(\alpha)\eta\left[\alpha,\frac{x+1}{2}\right] . \tag{C4}$$

The right-hand sides of Eqs. (C3) and (C4) yield the analytic continuation of the corresponding integrals as functions of α and x and thus provide the dimensional regularization for Eq. (C1) (see below).

For Dirichlet-Dirichlet boundary conditions, which correspond to the combination $(a,b)=(\mathcal{O},\mathcal{O})$ of surface universality classes, one finds from Eqs. (B4), (C1), and (C2)

$$\bar{e}^{(1)}_{\mathcal{O},\mathcal{O}}(0,z,L)=-\frac{N}{2}\int\frac{d^{d-1}p}{(2\pi)^{d-1}}\frac{\sinh pz\,\sinh p(L-z)}{p\,\sinh pL}$$
$$=-\frac{N}{2}\frac{\sqrt{\pi}}{2^d\pi^{d/2}}\frac{1}{\Gamma\left[\frac{d-1}{2}\right]}\int_0^\infty\frac{p^{d-3}}{\sinh pL}(e^{pL}-e^{p(2z-L)}-e^{p(L-2z)}+e^{-pL})dp .$$

With the substitutions $x=z/L$, $y=pL$, and by using Eq. (C3) one finally obtains

$$\bar{e}^{(1)}_{\mathcal{O},\mathcal{O}}(0,z,L)=\frac{N}{2}\frac{\Gamma\left[\frac{d}{2}-1\right]}{2^d\pi^{d/2}}L^{-(d-2)}[\zeta(d-2,z/L)+\zeta(d-2,1-z/L)-2\zeta(d-2)] , \tag{C5}$$

where $\zeta(d-2,0)=\zeta(d-2,1)=\zeta(d-2)$ in dimensional regularization [see Eq. (A3) for $p=1$] and the duplication formula for the Γ function

$$\Gamma(\alpha)=2^{\alpha-1}\pi^{-1/2}\Gamma\left[\frac{\alpha}{2}\right]\Gamma\left[\frac{\alpha+1}{2}\right] \tag{C6}$$

for $\alpha=d-2$ have been used.

Neumann-Neumann boundary conditions correspond to the pair $(a,b)=(SB,SB)$ of surface universality classes. From Eq. (B5) we conclude that

$$\bar{e}^{(1)}_{SB,SB}(0,z,L)=-\frac{N}{2}\int\frac{d^{d-1}p}{(2\pi)^{d-1}}\frac{\cosh pz\,\cosh p(L-z)}{p\,\sinh pL}$$
$$=-\frac{N}{2}\frac{\sqrt{\pi}}{2^d\pi^{d/2}}\frac{1}{\Gamma\left[\frac{d-1}{2}\right]}\int_0^\infty\frac{p^{d-3}}{\sinh pL}(e^{pL}+e^{p(2z-L)}+e^{p(L-2z)}+e^{-pL})dp .$$

In direct analogy with Eq. (C5) the result reads

$$\bar{e}^{(1)}_{SB,SB}(0,z,L)=-\frac{N}{2}\frac{\Gamma\left[\frac{d}{2}-1\right]}{2^d\pi^{d/2}}L^{-(d-2)}[\zeta(d-2,z/L)+\zeta(d-2,1-z/L)+2\zeta(d-2)] . \tag{C7}$$

Dirichlet-Neumann boundary conditions, i.e., $(a,b)=(\mathcal{O},SB)$ lead to the one-loop contribution

$$\bar{e}^{(1)}_{\mathcal{O},SB}(0,z,L)=-\frac{N}{2}\int\frac{d^{d-1}p}{(2\pi)^{d-1}}\frac{\sinh pz\,\cosh p(L-z)}{p\,\cosh pL}$$
$$=-\frac{N}{2}\frac{\sqrt{\pi}}{2^d\pi^{d/2}}\frac{1}{\Gamma\left[\frac{d-1}{2}\right]}\int_0^\infty\frac{p^{d-3}}{\cosh pL}(e^{pL}+e^{p(2z-L)}-e^{p(L-2z)}-e^{-pL})dp$$

to the bare energy density profile $\bar{e}_{\mathcal{O},SB}(0,z,L)$. Here Eq. (C4) and the substitutions $x=z/L$ and $y=pL$ establish the final result

$$\bar{e}^{(1)}_{\mathcal{O},SB}(0,z,L)=\frac{N}{2}\frac{\Gamma\left[\frac{d}{2}-1\right]}{2^d\pi^{d/2}}L^{-(d-2)}[\eta(d-2,z/L)-\eta(d-2,1-z/L)+2\eta(d-2)] , \tag{C8}$$

where $\eta(d-2,0)=-\eta(d-2,1)=-\eta(d-2)$ in dimensional regularization [see Eq. (A3) for $p=-1$] and Eq. (C6) has been used for $\alpha=d-2$. For $(a,b)=(SB,\mathcal{O})$ we note that $\bar{e}^{(1)}_{SB,\mathcal{O}}(0,z,L)=\bar{e}^{(1)}_{\mathcal{O},SB}(0,L-z,L)$.

As expected, periodic and antiperiodic boundary conditions yield constant energy density profiles. To one-loop order one has for periodic boundary conditions [see Eqs. (B7), (C1), and (C2)]

$$\bar{e}^{(1)}_{\rm per}(0,z,L)=-\frac{N}{2}\int\frac{d^{d-1}p}{(2\pi)^{d-1}}\frac{\cosh\frac{1}{2}pL}{2p\sinh\frac{1}{2}pL}$$
$$=-\frac{N}{2}\frac{\sqrt{\pi}}{2^d\pi^{d/2}}\frac{1}{\Gamma\left[\frac{d-1}{2}\right]}\int_0^\infty\frac{p^{d-3}}{\sinh\frac{1}{2}pL}(e^{pL/2}+e^{-pL/2})dp\ .$$

The substitution $x=\frac{1}{2}pL$, Eq. (C3), the dimensional regularization $\zeta(d-2,0)=\zeta(d-2)$, and Eq. (C6) for $\alpha=d-2$ lead to the final result

$$\bar{e}^{(1)}_{\rm per}(0,z,L)=-N\frac{\Gamma\left[\frac{d}{2}-1\right]}{2^d\pi^{d/2}}L^{-(d-2)}2^{d-2}\zeta(d-2)\ . \tag{C9}$$

Likewise, one obtains for antiperiodic boundary conditions

$$\bar{e}^{(1)}_{\rm aper}(0,z,L)=-\frac{N}{2}\int\frac{d^{d-1}p}{(2\pi)^{d-1}}\frac{\sinh\frac{1}{2}pL}{2p\cosh\frac{1}{2}pL}$$
$$=-\frac{N}{2}\frac{\sqrt{\pi}}{2^d\pi^{d/2}}\frac{1}{\Gamma\left[\frac{d-1}{2}\right]}$$
$$\times\int_0^\infty\frac{p^{d-3}}{\cosh\frac{1}{2}pL}(e^{pL/2}-e^{-pL/2})dp$$

so that Eq. (C4) and the dimensional regularization $\eta(d-2,0)=-\eta(d-2)$ yield

$$\bar{e}^{(1)}_{\rm aper}(0,z,L)=N\frac{\Gamma\left[\frac{d}{2}-1\right]}{2^d\pi^{d/2}}L^{-(d-2)}2^{d-2}\eta(d-2)\ , \tag{C10}$$

in analogy with Eq. (C9).

APPENDIX D: TWO-LOOP CONTRIBUTIONS TO THE ENERGY DENSITY PROFILES

The two-loop contribution $\bar{e}^{(2)}_{a,b}(\tau,z,L)$ to the bare energy density profile $\bar{e}_{a,b}(\tau,z,L)$ is given by

$$\bar{e}^{(2)}_{a,b}(\tau,z,L)$$
$$=gN\frac{N+2}{12}\int_0^L dz'\int\frac{d^{d-1}p_1}{(2\pi)^{d-1}}[G^{(0)a,b}(\mathbf{p}_1;z,z')]^2$$
$$\times\int\frac{d^{d-1}p_2}{(2\pi)^{d-1}}G^{(0)a,b}$$
$$\times(\mathbf{p}_2;z',z')\ , \tag{D1}$$

where $G^{(0)a,b}(\mathbf{p};z,z')$ is defined by Eq. (C2) and by Eqs. (B4)–(B8). The second momentum integral in Eq. (D1) has already been evaluated in Appendix C for $\tau=0$ and all boundary conditions under consideration. In order to evaluate Eq. (D1) for $\tau=0$ we first calculate the integral over $[G^{(0)a,b}]^2$. First, we note that in analogy with Eqs. (C3) and (C4) the identities

$$\int_0^\infty\frac{y^{\alpha-1}e^{-xy}}{\sinh^2\frac{1}{2}y}=4\Gamma(\alpha)[\zeta(\alpha-1,x+1)-x\zeta(\alpha,x+1)] \tag{D2}$$

and

$$\int_0^\infty\frac{y^{\alpha-1}e^{-xy}}{\cosh^2\frac{1}{2}y}=4\Gamma(\alpha)[\eta(\alpha-1,x+1)-x\eta(\alpha,x+1)] \tag{D3}$$

hold, which provide the dimensional regularization for Eq. (D1) through their dependence on α. Furthermore, we have, according to Eq. (A3), for $x>0$

$$\zeta(\alpha-1,x+1)-x\zeta(\alpha,x+1)=\zeta(\alpha-1,x)-x\zeta(\alpha,x) \tag{D4}$$

and

$$\eta(\alpha-1,x+1)-x\eta(\alpha,x+1)=x\eta(\alpha,x)-\eta(\alpha-1,x)\ . \tag{D5}$$

From Eqs. (D2), (D4), and (D5) we obtain for $D-D$ and $N-N$ boundary conditions

$$\int \frac{d^{d-1}p}{(2\pi)^{d-1}}[G^{(0)a,a}(\mathbf{p};z,z')]^2 = \frac{1}{2^d\pi^{d/2}} \frac{\Gamma\left[\frac{d}{2}-1\right]}{d-3} L^{-(d-3)}$$
$$\times[\zeta(d-4,|x-x'|)+\zeta(d-4,1-|x-x'|)$$
$$+(1-|x-x'|)[\zeta(d-3,|x-x'|)-\zeta(d-3,1-|x-x'|)]$$
$$+\zeta(d-4,x+x')+\zeta(d-4,2-x-x')$$
$$+(1-x-x')[\zeta(d-3,x+x')-\zeta(d-3,2-x-x')]$$
$$\mp 2\{\zeta(d-4,\tfrac{1}{2}(x+x'-|x-x'|))+\zeta(d-4,1-\tfrac{1}{2}(x+x'-|x-x'|))$$
$$-\tfrac{1}{2}(x+x'-|x-x'|)$$
$$\times[\zeta(d-3,\tfrac{1}{2}(x+x'-|x-x'|))-\zeta(d-3,1-\tfrac{1}{2}(x+x'-|x-x'|))]$$
$$+\zeta(d-4,\tfrac{1}{2}(x+x'+|x-x'|))+\zeta(d-4,1-\tfrac{1}{2}(x+x'+|x-x'|))$$
$$+[1-\tfrac{1}{2}(x+x'+|x-x'|)]$$
$$\times[\zeta(d-3,\tfrac{1}{2}(x+x'+|x-x'|))$$
$$-\zeta(d-3,1-\tfrac{1}{2}(x+x'+|x-x'|))]\}+4\zeta(d-4)]\,, \tag{D6}$$

where the upper and the lower signs correspond to $a=D$ and N, respectively, and $x=z/L$, $x'=z'/L$. For $D-N$ boundary conditions one obtains from Eqs. (D3)–(D5) the corresponding result

$$\int \frac{d^{d-1}p}{(2\pi)^{d-1}}[G^{(0)D,N}(\mathbf{p};z,z')]^2 = \frac{-1}{2^d\pi^{d/2}} \frac{\Gamma\left[\frac{d}{2}-1\right]}{d-3} L^{-(d-3)}$$
$$\times[\eta(d-4,1-|x-x'|)-\eta(d-4,|x-x'|)$$
$$-(1-|x-x'|)[\eta(d-3,|x-x'|)+\eta(d-3,1-|x-x'|)]$$
$$-\eta(d-4,x+x')-\eta(d-4,2-x-x')$$
$$-(1-x-x')[\eta(d-3,x+x')-\eta(d-3,2-x-x')]$$
$$+2\{\eta(d-4,\tfrac{1}{2}(x+x'-|x-x'|))-\eta(d-4,1-\tfrac{1}{2}(x+x'-|x-x'|))$$
$$-\tfrac{1}{2}(x+x'-|x-x'|)[\eta(d-3,\tfrac{1}{2}(x+x'-|x-x'|))$$
$$+\eta(d-3,1-\tfrac{1}{2}(x+x'-|x-x'|))]$$
$$+\eta(d-4,\tfrac{1}{2}(x+x'+|x-x'|))$$
$$-\eta(d-4,1-\tfrac{1}{2}(x+x'+|x-x'|))$$
$$+[1-\tfrac{1}{2}(x+x'+|x-x'|)]$$
$$\times[\eta(d-3,\tfrac{1}{2}(x+x'+|x-x'|))$$
$$+\eta(d-3,1-\tfrac{1}{2}(x+x'+|x-x'|))]\}+4\eta(d-4)]\,. \tag{D7}$$

Finally, Eqs. (D2) and (D3) lead to

$$\int \frac{d^{d-1}p}{(2\pi)^{d-1}}[G^{(0)\mathrm{per}}(\mathbf{p};z,z')]^2 = \frac{1}{2^d\pi^{d/2}} \frac{\Gamma\left[\frac{d}{2}-1\right]}{d-3} \left[\frac{L}{2}\right]^{-(d-3)}$$
$$\times\{\zeta(d-4,2|x-x'|)+\zeta(d-4,2-2|x-x'|)$$
$$+(1-2|x-x'|)[\zeta(d-3,2|x-x'|)-\zeta(d-3,2-2|x-x'|)]+2\zeta(d-4)\} \tag{D8}$$

for periodic boundary conditions and to

$$\int \frac{d^{d-1}p}{(2\pi)^{d-1}}[G^{(0)\mathrm{aper}}(\mathbf{p};z,z')]^2=\frac{1}{2^d\pi^{d/2}}\frac{\Gamma\left[\frac{d}{2}-1\right]}{d-3}\left[\frac{L}{2}\right]^{-(d-3)} \times\{\eta(d-4,2|x-x'|)+\eta(d-4,2-2|x-x'|) +(1-2|x-x'|)[\eta(d-3,2|x-x'|)-\eta(d-3,2-2|x-x'|)]-2\eta(d-4)\} \quad \text{(D9)}$$

for antiperiodic boundary conditions. In order to perform the remaining integration over z' in Eq. (D1) in a systematic way we decompose the integral into four parts. For $D-D$, $N-N$, and $D-N$ boundary conditions we define

$$\begin{aligned} I_1^{a,b}(x)&=\int_0^1 P^{a,b}(x')Q_1^{a,b}(|x-x'|)dx' ,\\ I_2^{a,b}(x)&=\int_0^1 P^{a,b}(x')Q_1^{a,b}(x+x')dx' ,\\ I_3^{a,b}(x)&=\int_0^1 P^{a,b}(x')Q_3^{a,b}(x,x')dx' ,\\ I_4^{a,b}&=\int_0^1 P^{a,b}(x')Q_4^{a,b}dx' , \end{aligned} \quad \text{(D10)}$$

where we have used the abbreviations

$$\begin{aligned} P^{D,D}(x)&=\zeta(d-2,x)+\zeta(d-2,1-x)-2\zeta(d-2) ,\\ P^{N,N}(x)&=\zeta(d-2,x)+\zeta(d-2,1-x)+2\zeta(d-2) ,\\ P^{D,N}(x)&=\eta(d-2,x)-\eta(d-2,1-x)+2\eta(d-2) , \end{aligned} \quad \text{(D11)}$$

and

$$\begin{aligned} Q_1^{a,a}(x)&=\zeta(d-4,x)+\zeta(d-4,1-x)+(1-x)[\zeta(d-3,x)-\zeta(d-3,1-x)] ,\\ Q_1^{D,N}(x)&=\eta(d-4,1-x)-\eta(d-4,x)-(1-x)[\eta(d-3,x)+\eta(d-3,1-x)] ,\\ Q_3^{a,a}(x,x')&=\zeta(d-4,x)+\zeta(d-4,1-x)-x[\zeta(d-3,x)-\zeta(d-3,1-x)]\\ &\quad+\zeta(d-4,x')+\zeta(d-4,1-x')-x'[\zeta(d-3,x')-\zeta(d-3,1-x')]\\ &\quad+\zeta(d-3,\tfrac{1}{2}(x+x'+|x-x'|))-\zeta(d-3,1-\tfrac{1}{2}(x+x'+|x-x'|)) ,\\ Q_3^{D,N}(x,x')&=\eta(d-4,x)-\eta(d-4,1-x)-x[\eta(d-3,x)+\eta(d-3,1-x)]\\ &\quad+\eta(d-4,x')-\eta(d-4,1-x')-x'[\eta(d-3,x')+\eta(d-3,1-x')]\\ &\quad+\eta(d-3,\tfrac{1}{2}(x+x'+|x-x'|))+\eta(d-3,1-\tfrac{1}{2}(x+x'+|x-x'|)) ,\\ Q_4^{a,a}&=4\zeta(d-4) ,\\ Q_4^{D,N}&=4\eta(d-4) \end{aligned} \quad \text{(D12)}$$

for $a=D$ and N. In obtaining Eq. (D12) we have used the identity

$$f(\tfrac{1}{2}(x+x'-|x-x'|)) +f(\tfrac{1}{2}(x+x'+|x-x'|))=f(x)+f(x') .$$

Furthermore, we note that

$$\begin{aligned} Q_1^{a,a}(x)&=\zeta(d-4,x)+\zeta(d-4,2-x)\\ &\quad+(1-x)[\zeta(d-3,x)-\zeta(d-3,2-x)] ,\\ Q_1^{D,N}(x)&=-\eta(d-4,2-x)-\eta(d-4,x)\\ &\quad-(1-x)[\eta(d-3,x)-\eta(d-3,2-x)] , \end{aligned} \quad \text{(D13)}$$

which is a direct consequence of Eqs. (D4) and (D5). Using Eqs. (D10)–(D12) one obtains the following representations for the two-loop contributions $\bar{e}^{(2)}_{a,b}(0,z,L)$ to the bare energy density profile $\bar{e}_{a,b}(0,z,L)$:

$$\bar{e}^{(2)}_{\mathcal{O},\mathcal{O}}(0,z,L)=-gN\frac{N+2}{12}\frac{\Gamma^2\left[\frac{d}{2}-1\right]}{2^{2d}\pi^d}\frac{L^{-2(d-3)}}{d-3}\times[I_1^{D,D}(x)+I_2^{D,D}(x)-2I_3^{D,D}(x)+I_4^{D,D}]\ ,$$

$$\bar{e}^{(2)}_{\mathcal{O},SB}(0,z,L)=gN\frac{N+2}{12}\frac{\Gamma^2\left[\frac{d}{2}-1\right]}{2^{2d}\pi^d}\frac{L^{-2(d-3)}}{d-3}\times[I_1^{D,N}(x)+I_2^{D,N}(x)+2I_3^{D,N}(x)+I_4^{D,N}]\ ,\qquad\text{(D14)}$$

$$\bar{e}^{(2)}_{SB,SB}(0,z,L)=gN\frac{N+2}{12}\frac{\Gamma^2\left[\frac{d}{2}-1\right]}{2^{2d}\pi^d}\frac{L^{-2(d-3)}}{d-3}\times[I_1^{N,N}(x)+I_2^{N,N}(x)+2I_3^{N,N}(x)+I_4^{N,N}]\ .$$

For $\bar{e}^{(2)}_{\text{per}}$ and $\bar{e}^{(2)}_{\text{aper}}$ the above decomposition is not necessary. Using Eqs. (D8) and (D9) and Eq. (A4) for $p=\pm1$, Eq. (D1) can be evaluated directly in these two cases (see below).

In order to evaluate analytically the integrals listed in Eq. (D10), in the following we restrict ourselves to $d=4-\varepsilon$ and apply the ε expansion, where contributions of order ε can be disregarded. We first discuss the evaluation of Eq. (D10) for Dirichlet-Dirichlet boundary conditions in some detail; the remaining boundary conditions can then be treated along the same line of argument.

Starting with $I_1^{a,b}(x)$ we first note that

$$I_1^{a,b}(x)=\int_0^x P^{a,b}(x')Q_1^{a,b}(x-x')dx'+\int_0^{1-x}P^{a,b}(1-x')Q_1^{a,b}(1-x-x')dx'\ .\qquad\text{(D15)}$$

For $a=b=D,N$ one has from Eq. (D11) $P^{a,a}(1-x)=P^{a,a}(x)$ and therefore Eq. (D15) can be written in the form

$$I_1^{a,a}(x)=F_1^{a,a}(x)+F_1^{a,a}(1-x)\ .\qquad\text{(D16)}$$

Specifically, $F_1^{D,D}(x)$ is given by

$$F_1^{D,D}(x)=\int_0^x dx'\{\zeta(2-\varepsilon,x')+\zeta(2-\varepsilon,1-x')-2\zeta(2-\varepsilon)\}\times\{\zeta(-\varepsilon,x-x')+\zeta(-\varepsilon,1-(x-x'))+[1-(x-x')][\zeta(1-\varepsilon,x-x')-\zeta(1-\varepsilon,1-(x-x'))]\}\ ,\qquad\text{(D17)}$$

where [32]

$$\zeta(-\varepsilon,x)=\frac{1}{2}-x-\varepsilon\ln\frac{\Gamma(x)}{\sqrt{2\pi}}+O(\varepsilon^2)\qquad\text{(D18)}$$

so that

$$\zeta(-\varepsilon,x)+\zeta(-\varepsilon,1-x)=\varepsilon\ln(2\sin\pi x)+O(\varepsilon^2)\ .\qquad\text{(D19)}$$

For convenience we represent Eq. (D17) as a sum of three parts. Using Eq. (D19) one has for the first part

$$\begin{aligned}F_{1,1}^{D,D}(x)&=\int_0^x dx'[\zeta(2-\varepsilon,x')+\zeta(2-\varepsilon,1-x')-2\zeta(2-\varepsilon)][\zeta(-\varepsilon,x-x')+\zeta(-\varepsilon,1-(x-x'))]\\&=\int_0^x x'^{\varepsilon-2}[\zeta(-\varepsilon,x-x')+\zeta(-\varepsilon,1-(x-x'))]dx'+O(\varepsilon)\\&=\int_0^x x'^{\varepsilon-2}(x-x')^{\varepsilon}dx'+\int_0^x x'^{\varepsilon-2}[\zeta(-\varepsilon,1+x-x')+\zeta(-\varepsilon,1-(x-x'))]dx'+O(\varepsilon)\\&=x^{2\varepsilon-1}B(\varepsilon-1,\varepsilon+1)+2\zeta(-\varepsilon)\frac{x^{\varepsilon-1}}{\varepsilon-1}+\frac{1}{\varepsilon-1}[\zeta(1-\varepsilon,1+x)-\zeta(1-\varepsilon,1-x)]+O(\varepsilon)\end{aligned}\qquad\text{(D20)}$$

in dimensional regularization according to Eq. (A4) for $p=1$. The first derivative of Eq. (D19) with respect to x yields

$$\zeta(1-\varepsilon,x)-\zeta(1-\varepsilon,1-x)=\pi\cot\pi x+O(\varepsilon)\qquad\text{(D21)}$$

and we therefore obtain the ε expansion

$$F_{1,1}^{D,D}(x)=-\pi\cot\pi x+O(\varepsilon)\ .\qquad\text{(D22)}$$

The second part of $F_1^{D,D}(x)$ is chosen as

$$F_{1,2}^{D,D}(x)=\int_0^x dx'[\zeta(2-\varepsilon,x')+\zeta(2-\varepsilon,1-x')](1-x+x')[\zeta(1-\varepsilon,x-x')-\zeta(1-\varepsilon,1-(x-x'))] \ . \tag{D23}$$

The additional factor x' in the integrand of Eq. (D23) can be abolished by an integration by parts with respect to $\zeta(2-\varepsilon,x')+\zeta(2-\varepsilon,1-x')$, which leads to the alternative representation

$$F_{1,2}^{D,D}(x)=\left[1-\frac{x}{2}\right]\int_0^x dx'[\zeta(1-\varepsilon,x-x')-\zeta(1-\varepsilon,1-(x-x'))][\zeta(2-\varepsilon,x')+\zeta(2-\varepsilon,1-x')]$$
$$+\frac{1}{2(1-\varepsilon)}\int_0^x dx'[\zeta(1-\varepsilon,x-x')-\zeta(1-\varepsilon,1-(x-x'))][\zeta(1-\varepsilon,x')-\zeta(1-\varepsilon,1-x')] \tag{D24}$$

for $F_{1,2}^{D,D}(x)$. Using the identities [see Eq. (D21)]

$$\zeta(2,x)+\zeta(2,1-x)=\frac{\pi^2}{\sin^2\pi x}, \quad \zeta(3,x)-\zeta(3,1-x)=\frac{\pi^3\cos\pi x}{\sin^3\pi x} \ , \tag{D25}$$

Eq. (D24) can be evaluated up to terms of order ε in the same way as shown in Eq. (D20), although the calculation is more involved here. The result reads

$$F_{1,2}^{D,D}(x)=\left[1-\frac{x}{2}\right]\left\{\frac{2}{\varepsilon}[\zeta(2-\varepsilon,x)+\zeta(2-\varepsilon,1-x)]+2\frac{\ln x-1}{x^2}+4\zeta(2)\ln x-4\int_0^x \ln(x-x')\left[\frac{\pi^3\cos\pi x'}{\sin^3\pi x'}-\frac{1}{x'^3}\right]dx'\right.$$
$$\left.+\int_0^x\left[\pi\cot\pi(x-x')-\frac{1}{x-x'}\right]\left[\frac{\pi^2}{\sin^2\pi x'}-\frac{1}{x'^2}\right]dx'\right\}$$
$$+\frac{1}{2(1-\varepsilon)}\left\{\frac{2}{\varepsilon}[\zeta(1-\varepsilon,x)-\zeta(1-\varepsilon,1-x)]+2\frac{\ln x}{x^2}-2\int_0^x \ln(x-x')\left[\frac{\pi^2}{\sin^2\pi x'}-\frac{1}{x'^2}\right]dx'\right.$$
$$\left.+\int_0^x\left[\pi\cot\pi(x-x')-\frac{1}{x-x'}\right]\left[\pi\cot\pi x'-\frac{1}{x'}\right]dx'\right\}+O(\varepsilon) \ . \tag{D26}$$

The remainder of $F_1^{D,D}(x)$ is captured by the third part

$$F_{1,3}^{D,D}(x)=-2\zeta(2-\varepsilon)\int_0^x[1-(x-x')][\zeta(1-\varepsilon,x-x')-\zeta(1-\varepsilon,1-(x-x'))]dx' \ , \tag{D27}$$

which can be evaluated directly by integrating by parts giving

$$F_{1,3}^{D,D}(x)=2\zeta(2-\varepsilon)\left[\frac{2}{\varepsilon}\zeta(-\varepsilon)-(1-x)\ln(2\sin\pi x)-\frac{\zeta(-\varepsilon-1,x)-\zeta(-\varepsilon-1,1-x)}{\varepsilon(\varepsilon+1)}\right] \ . \tag{D28}$$

In shorthand notation we therefore find for $I_1^{D,D}(x)$ [see Eq. (D16)]

$$I_1^{D,D}(x)=\frac{8}{\varepsilon}\zeta(-\varepsilon)\zeta(2-\varepsilon)-2\zeta(2)\ln(2\sin\pi x)+F_{1,2}^{D,D}(x)+F_{1,2}^{D,D}(1-x)+O(\varepsilon) \ , \tag{D29}$$

where $F_{1,2}^{D,D}(x)$ is given by Eq. (D26).

We now turn to the second integral $I_2^{D,D}(x)$ [see Eq. (D10)], which is given by

$$I_2^{D,D}(x)=\int_0^1 dx'\{\zeta(2-\varepsilon,x')+\zeta(2-\varepsilon,1-x')-2\zeta(2-\varepsilon)\}$$
$$\times\{\zeta(-\varepsilon,x+x')+\zeta(-\varepsilon,2-x-x')+(1-x-x')[\zeta(1-\varepsilon,x+x')-\zeta(1-\varepsilon,2-x-x')]\} \ , \tag{D30}$$

where Eq. (D13) has been used. In analogy with Eq. (D17) we decompose Eq. (D30) into three parts. The first part is defined as

$$F_{2,1}^{D,D}(x)=\int_0^1 dx'[\zeta(2-\varepsilon,x')+\zeta(2-\varepsilon,1-x')-2\zeta(2-\varepsilon)][\zeta(-\varepsilon,x+x')+\zeta(-\varepsilon,2-x-x')] \ . \tag{D31}$$

Following the procedure sketched in Eq. (D20) we find

$$F_{2,1}^{D,D}(x)=\frac{1}{x}+\frac{1}{1-x}+2\zeta(2)+O(\varepsilon) \ . \tag{D32}$$

The second contribution to Eq. (D30) is written conveniently as $F_{2,2}^{D,D}(x)+F_{2,2}^{D,D}(1-x)$, where

$$F_{2,2}^{D,D}(x)=\int_0^x dx'[\zeta(2-\varepsilon,x')+\zeta(2-\varepsilon,1-x')](x-x')[\zeta(1-\varepsilon,1-x+x')-\zeta(1-\varepsilon,1+x-x')] \ . \tag{D33}$$

Due to the similarities between Eqs. (D33) and (D23) we skip the details of the calculation and quote only the result

$$F_{2,2}^{D,D}(x)=\frac{1}{\varepsilon}[\zeta(1-\varepsilon,x)-\zeta(1-\varepsilon,1-x)]-\frac{x}{\varepsilon}[\zeta(2-\varepsilon,x)+\zeta(2-\varepsilon,1-x)]$$
$$-2\zeta(2)x\ln x+\int_0^x[1-\pi(x-x')\cot\pi(x-x')]\left[\frac{\pi^2}{\sin^2\pi x'}-\frac{1}{x'^2}\right]dx'$$
$$-\int_0^x \ln(x-x')\left[\frac{\pi^2}{\sin^2\pi x'}-\frac{1}{x'^2}\right]dx'+2x\int_0^x \ln(x-x')\left[\frac{\pi^3\cos\pi x'}{\sin^3\pi x'}-\frac{1}{x'^3}\right]dx'+O(\varepsilon)\ . \tag{D34}$$

The last contribution to Eq. (D30) is given by

$$F_{2,3}^{D,D}(x)=2\zeta(2-\varepsilon)\int_0^x(x'+x-1)[\zeta(1-\varepsilon,x+x')-\zeta(1-\varepsilon,2-x-x')]dx'\ , \tag{D35}$$

which is similar to Eq. (D27). Integration by parts in dimensional regularization yields

$$F_{2,3}^{D,D}(x)=2\zeta(2)[\ln(2\sin\pi x)-1]+O(\varepsilon)\ , \tag{D36}$$

so that we obtain for $I_2^{D,D}(x)$ in shorthand notation

$$I_2^{D,D}(x)=2\zeta(2)\ln(2\sin\pi x)+\frac{1}{x}+\frac{1}{1-x}+F_{2,2}^{D,D}(x)+F_{2,2}^{D,D}(1-x)+O(\varepsilon)\ , \tag{D37}$$

where $F_{2,2}^{D,D}(x)$ is given by Eq. (D34).

According to Eqs. (D10)–(D12) we have for the third integral $I_3^{D,D}(x)$

$$I_3^{D,D}(x)=\int_0^1 dx'\{\zeta(2-\varepsilon,x')+\zeta(2-\varepsilon,1-x')-2\zeta(2-\varepsilon)\}$$
$$\times\{\zeta(-\varepsilon,x)+\zeta(-\varepsilon,1-x)-x[\zeta(1-\varepsilon,x)-\zeta(1-\varepsilon,1-x)]$$
$$+\zeta(-\varepsilon,x')+\zeta(-\varepsilon,1-x')-x'[\zeta(1-\varepsilon,x')-\zeta(1-\varepsilon,1-x')]$$
$$+\zeta(1-\varepsilon,\tfrac{1}{2}(x+x'+|x-x'|))-\zeta(1-\varepsilon,1-\tfrac{1}{2}(x+x'+|x-x'|))\}\ , \tag{D38}$$

which is again decomposed into three contributions. The first contribution is defined as

$$F_{3,1}^{D,D}(x)=\int_0^1 dx'\{\zeta(2-\varepsilon,x')+\zeta(2-\varepsilon,1-x')-2\zeta(2-\varepsilon)\}$$
$$\times\{\zeta(-\varepsilon,x)+\zeta(-\varepsilon,1-x)-x[\zeta(1-\varepsilon,x)-\zeta(1-\varepsilon,1-x)]\}\ . \tag{D39}$$

According to Eq. (A6) we find for $F_{3,1}^{D,D}(x)$ in dimensional regularization

$$F_{3,1}^{D,D}(x)=-2\zeta(2-\varepsilon)\{\zeta(-\varepsilon,x)+\zeta(-\varepsilon,1-x)-x[\zeta(1-\varepsilon,x)-\zeta(1-\varepsilon,1-x)]\}$$
$$=2\zeta(2)\pi x\cot\pi x+O(\varepsilon)\ , \tag{D40}$$

where Eqs. (D19) and (D21) have been used. The second contribution to $I_3^{D,D}(x)$ is defined as

$$F_{3,2}^{D,D}(x)=\int_0^1 dx'\{\zeta(2-\varepsilon,x')+\zeta(2-\varepsilon,1-x')-2\zeta(2-\varepsilon)\}$$
$$\times\{\zeta(-\varepsilon,x')+\zeta(-\varepsilon,1-x')-x'[\zeta(1-\varepsilon,x')-\zeta(1-\varepsilon,1-x')]\}\ . \tag{D41}$$

Noting that due to an integration by parts one has

$$\int_0^1 dx'x'[\zeta(1-\varepsilon,x')-\zeta(1-\varepsilon,1-x')][\zeta(2-\varepsilon,x')+\zeta(2-\varepsilon,1-x')]=-\frac{1}{2(1-\varepsilon)}\int_0^1 dx'[\zeta(1-\varepsilon,x')-\zeta(1-\varepsilon,1-x')]^2\ ,$$

Eq. (D41) can be evaluated in closed form using Eqs. (A8a), (A8b), (A12a), and (A12b). For brevity we quote only the ε-expanded result

$$F_{3,2}^{D,D}(x)=\frac{4}{\varepsilon}\zeta(-\varepsilon)\zeta(2-\varepsilon)+\frac{\pi^2}{2}+O(\varepsilon)\ . \tag{D42}$$

The remainder of Eq. (D38) is collected in the last contribution

$$F_{3,3}^{D,D}(x)=\int_0^1 dx'\{\zeta(2-\varepsilon,x')+\zeta(2-\varepsilon,1-x')-2\zeta(2-\varepsilon)\}$$
$$\times\{\zeta(1-\varepsilon,\tfrac{1}{2}(x+x'+|x-x'|))-\zeta(1-\varepsilon,1-\tfrac{1}{2}(x+x'+|x-x'|))\}\ . \tag{D43}$$

Noting that

$$\zeta(2-\varepsilon,x)+\zeta(2,1-x)=\frac{1}{\varepsilon-1}\frac{\partial}{\partial x}[\zeta(1-\varepsilon,x)-\zeta(1-\varepsilon,1-x)]$$

[see Eq. (A4)], we find for $F_{3,3}^{D,D}(x)$

$$F_{3,3}^{D,D}(x)=-\frac{4}{\varepsilon}\zeta(-\varepsilon)\zeta(2-\varepsilon)-\frac{\pi^2}{2}\cot^2\pi x-2\zeta(2)\pi x\cot\pi x+2\zeta(2)\ln(2\sin\pi x)+O(\varepsilon)\ , \tag{D44}$$

which finally yields

$$I_3^{D,D}(x)=\frac{\pi^2}{2}(1-\cot^2\pi x)+2\zeta(2)\ln(2\sin\pi x)+O(\varepsilon)\ . \tag{D45}$$

The last integral in Eq. (D10) is simple and yields

$$I_4^{D,D}=4\zeta(-\varepsilon)\int_0^1 dx'[\zeta(2-\varepsilon,x')+\zeta(2-\varepsilon,1-x')-2\zeta(2-\varepsilon)]$$

$$=-8\zeta(-\varepsilon)\zeta(2-\varepsilon)=4\zeta(2)+O(\varepsilon)\ , \tag{D46}$$

where only Eq. (A6) has been used. Collecting the additional terms from Eqs. (D29), (D37), and (D45) one finds, according to Eq. (D14),

$$\bar{e}_{\mathcal{O},\mathcal{O}}^{(2)}(0,z,L)=-gN\frac{N+2}{12}\frac{\Gamma^2\left(\frac{d}{2}-1\right)}{2^{2d}\pi^d}\frac{L^{-2(1-\varepsilon)}}{1-\varepsilon}$$

$$\times\left\{\frac{8}{\varepsilon}\zeta(-\varepsilon)\zeta(2-\varepsilon)-4\zeta(2)\ln(2\sin\pi x)-\pi^2(1-\cot^2\pi x)+\frac{1}{x}+\frac{1}{1-x}\right.$$

$$\left.+4\zeta(2)+F_{1,2}^{D,D}(x)+F_{1,2}^{D,D}(1-x)+F_{2,2}^{D,D}(x)+F_{2,2}^{D,D}(1-x)\right\}\ . \tag{D47}$$

In order to evaluate Eq. (D47) further we note that according to Eqs. (D26) and (D34) we have

$$F_{1,2}^{D,D}(x)+F_{1,2}^{D,D}(1-x)+F_{2,2}^{D,D}(x)+F_{2,2}^{D,D}(1-x)$$

$$=\frac{2}{\varepsilon}[\zeta(2-\varepsilon,x)+\zeta(2-\varepsilon,1-x)]+2\frac{\ln x-1}{x^2}+2\frac{\ln(1-x)-1}{(1-x)^2}+\frac{1}{x}+\frac{1}{1-x}$$

$$+4\zeta(2)[(1-x)\ln x+x\ln(1-x)]+J^{D,D}(x)+J^{D,D}(1-x)+O(\varepsilon)\ , \tag{D48}$$

where

$$J^{D,D}(x)=-4(1-x)J_1^{D,D}(x)+\left[1-\frac{x}{2}\right]J_2^{D,D}(x)+J_3^{D,D}(x)+\frac{1}{2}J_4^{D,D}(x)-2J_5^{D,D}(x) \quad \text{(D49)}$$

and

$$\begin{aligned}
J_1^{D,D}(x)&=\int_0^x \ln(x-x')\left[\frac{\pi^3\cos\pi x'}{\sin^3\pi x'}-\frac{1}{x'^3}\right]dx' ,\\
J_2^{D,D}(x)&=\int_0^x \left[\pi\cot\pi(x-x')-\frac{1}{x-x'}\right]\times\left[\frac{\pi^2}{\sin^2\pi x'}-\frac{1}{x'^2}\right]dx' ,\\
J_3^{D,D}(x)&=\int_0^x [1-\pi(x-x')\cot\pi(x-x')]\times\left[\frac{\pi^2}{\sin^2\pi x'}-\frac{1}{x'^2}\right]dx' ,\\
J_4^{D,D}(x)&=\int_0^x \left[\pi\cot\pi(x-x')-\frac{1}{x-x'}\right]\times\left[\pi\cot\pi x'-\frac{1}{x'}\right]dx' ,\\
J_5^{D,D}(x)&=\int_0^x \ln(x-x')\left[\frac{\pi^2}{\sin^2\pi x'}-\frac{1}{x'^2}\right]dx' ,
\end{aligned} \quad \text{(D50)}$$

as can be read off directly from Eqs. (D26) and (D34). The first three integrals listed in Eq. (D50) can be expressed by $J_4^{D,D}(x)$ and $J_5^{D,D}(x)$ via

$$\begin{aligned}
J_1^{D,D}(x)&=\zeta(2)\ln x-\tfrac{1}{2}[J_5^{D,D}(x)]' ,\\
J_2^{D,D}(x)&=-[J_4^{D,D}(x)]' ,\\
J_3^{D,D}(x)&=\tfrac{1}{2}[xJ_4^{D,D}(x)]' ,
\end{aligned} \quad \text{(D51)}$$

where the prime denotes the derivative with respect to x. The calculation of $J_4^{D,D}(x)$ and $J_5^{D,D}(x)$ can be conveniently performed using the series representation

$$\pi\cot\pi x=\frac{1}{x}+\sum_{n\neq 0}\left[\frac{1}{x+n}-\frac{1}{n}\right] , \quad \text{(D52)}$$

from which further useful identities follow by integrating or differentiating with respect to x. One obtains

$$\begin{aligned}
J_4^{D,D}(x)&=\pi^2x+2\pi\cot\pi x\ln\frac{\sin\pi x}{\pi x}-2\sum_{n\neq 0}\frac{\ln\left[1+\frac{x}{n}\right]}{x+n} ,\\
J_5^{D,D}(x)&=-\ln x\left[\pi\cot\pi x-\frac{1}{x}\right]-\sum_{n\neq 0}\frac{\ln\left[1+\frac{x}{n}\right]}{x+n} ,
\end{aligned} \quad \text{(D53)}$$

where the summations are to be carried out over all integers n except $n=0$. From Eqs. (D51) and (D53) simple algebra leads to an explicit expression for $J^{D,D}(x)$. Thus Eqs. (D47) and (D48) yield the final result

$$\bar{e}^{(2)}_{\mathcal{O},\mathcal{O}}(0,z,L)=-gN\frac{N+2}{12}\frac{\Gamma^2\left[\frac{d}{2}-1\right]}{2^{2d}\pi^d}\frac{L^{-2(1-\varepsilon)}}{1-\varepsilon}\left\{\frac{2}{\varepsilon}[\zeta(2-\varepsilon,x)+\zeta(2-\varepsilon,1-x)-2\zeta(2-\varepsilon)]+\frac{\pi^2}{\sin^2\pi x}-2\left[\frac{\pi^2}{\sin^2\pi x}-\frac{\pi^2}{3}\right]\left[1+\ln\frac{\pi}{\sin\pi x}\right]+O(\varepsilon)\right\} . \quad \text{(D54)}$$

The two-loop contribution $\bar{e}^{(2)}_{SB,SB}(0,z,L)$ to the bare energy density profile for Neumann-Neumann boundary conditions differs from $\bar{e}^{(2)}_{\mathcal{O},\mathcal{O}}(0,z,L)$ only in the *sign* of some contributions [see Eqs. (D6), (D11), and (D14)]. We therefore note only that

$$\bar{e}^{(2)}_{SB,SB}(0,z,L)=gN\frac{N+2}{12}\frac{\Gamma^2\left[\frac{d}{2}-1\right]}{2^{2d}\pi^d}\frac{L^{-2(1-\varepsilon)}}{1-\varepsilon}\left\{-\frac{8}{\varepsilon}\zeta(-\varepsilon)\zeta(2-\varepsilon)-4\zeta(2)\ln(2\sin\pi x)+\pi^2(1-\cot^2\pi x)+\frac{1}{x}+\frac{1}{1-x}-4\zeta(2)+F^{D,D}_{1,2}(x)+F^{D,D}_{1,2}(1-x)+F^{D,D}_{2,2}(x)+F^{D,D}_{2,2}(1-x)\right\} , \quad \text{(D55)}$$

which should be compared to Eq. (D47). From Eq. (D48) the final result

$$\bar{e}^{(2)}_{SB,SB}(0,z,L)=gN\frac{N+2}{12}\frac{\Gamma^2\left[\frac{d}{2}-1\right]}{2^{2d}\pi^d}\frac{L^{-2(1-\varepsilon)}}{1-\varepsilon}\left\{\frac{2}{\varepsilon}[\zeta(2-\varepsilon,x)+\zeta(2-\varepsilon,1-x)+2\zeta(2-\varepsilon)]-\frac{\pi^2}{\sin^2\pi x}-2\left[\frac{\pi^2}{\sin^2\pi x}-\frac{\pi^2}{3}\right]\left[1+\ln\frac{\pi}{\sin\pi x}\right]+\frac{4}{3}\pi^2(2-\ln 2\pi)+O(\varepsilon)\right\} \quad \text{(D56)}$$

can be obtained easily.

For $\bar{e}^{(2)}_{\mathcal{O},SB}(0,z,L)$, however, another calculation is required in which bivariate η functions replace the Hurwitz functions [see Eqs. (D7), (D11), and (D12)]. As shown in Appendix A, Hurwitz and bivariate η functions can be treated on the same footing so that the calculation follows the same route as for $\bar{e}^{(2)}_{\mathcal{O},\mathcal{O}}(0,z,L)$. We will therefore refrain from reproducing the details here and quote only the main results according to the above definitions. Starting from Eq. (D10) we note that

$$
\begin{aligned}
I_1^{D,N}(x)&=-\frac{8}{\varepsilon}\eta(-\varepsilon)\eta(2-\varepsilon)-2\eta(2)(1-2x)\ln\tan\frac{\pi}{2}x-4\eta(2)\int_0^x \ln\tan\frac{\pi}{2}t\,dt-F_1^{D,N}(x)+F_1^{D,N}(1-x)+O(\varepsilon)\ ,\\
I_2^{D,N}(x)&=-\frac{1}{x}+\frac{1}{1-x}+2\eta(2)(1-2x)\ln\tan\frac{\pi}{2}x+4\eta(2)\int_0^x \ln\tan\frac{\pi}{2}t\,dt+F_2^{D,N}(x)-F_2^{D,N}(1-x)+O(\varepsilon)\ ,\\
I_3^{D,N}(x)&=-\frac{1}{2}\frac{\pi^2}{\sin^2\pi x}-2\eta(2)\ln\tan\frac{\pi}{2}x+O(\varepsilon)\ ,\\
I_4^{D,N}&=4\eta(2)+O(\varepsilon)\ ,
\end{aligned}
\tag{D57}
$$

where

$$
\begin{aligned}
F_1^{D,N}(x)&=\left[1-\frac{x}{2}\right]\left\{\frac{2}{\varepsilon}[\eta(2-\varepsilon,x)-\eta(2-\varepsilon,1-x)]+2\frac{\ln x-1}{x^2}-4\eta(2)\ln x-4J_1^{D,N}(x)+J_2^{D,N}(x)\right\}\\
&\quad+\frac{1}{2(1-\varepsilon)}\left\{\frac{2}{\varepsilon}[\eta(1-\varepsilon,x)+\eta(1-\varepsilon,1-x)]+2\frac{\ln x}{x}-2J_3^{D,N}(x)+J_4^{D,N}(x)\right\}+O(\varepsilon)\ ,\\
F_2^{D,N}(x)&=-\frac{1}{\varepsilon}[\eta(1-\varepsilon,x)+\eta(1-\varepsilon,1-x)]+\frac{x}{\varepsilon}[\eta(2-\varepsilon,x)-\eta(2-\varepsilon,1-x)]\\
&\quad-2\eta(2)\ln x-2xJ_1^{D,N}(x)+\frac{x}{2}J_2^{D,N}(x)+J_3^{D,N}(x)-\frac{1}{2}J_4^{D,N}(x)+O(\varepsilon)\ .
\end{aligned}
\tag{D58}
$$

In Eqs. (D57) and (D58) we have used the identity

$$
\eta(-\varepsilon,x)-\eta(-\varepsilon,1-x)=-\varepsilon\ln\tan\frac{\pi}{2}x+O(\varepsilon^2)
\tag{D59}
$$

[see Eq. (D19)] and the abbreviations

$$
\begin{aligned}
J_1^{D,N}(x)&=\int_0^x \ln(x-x')\left[\frac{\pi^3}{\sin^3\pi x'}-\frac{\pi^2}{2}\frac{\pi}{\sin\pi x'}-\frac{1}{x'^3}\right]dx'\ ,\\
J_2^{D,N}(x)&=\int_0^x \left[\frac{\pi}{\sin\pi(x-x')}-\frac{1}{x-x'}\right]\left[\frac{\pi^2\cos\pi x'}{\sin^2\pi x'}-\frac{1}{x'^2}\right]dx'\ ,\\
J_3^{D,N}(x)&=\int_0^x \ln(x-x')\left[\frac{\pi^2\cos\pi x'}{\sin^2\pi x'}-\frac{1}{x'^2}\right]dx'\ ,\\
J_4^{D,N}(x)&=\int_0^x \left[\frac{\pi}{\sin\pi(x-x')}-\frac{1}{x-x'}\right]\left[\frac{\pi}{\sin\pi x'}-\frac{1}{x'}\right]dx'\ .
\end{aligned}
\tag{D60}
$$

From Eqs. (D14) and (D58) we thus find in analogy with Eqs. (D47) and (D48)

$$\bar{e}^{(2)}_{\mathcal{O},SB}(0,z,L)=gN\frac{N+2}{12}\frac{\Gamma^2\left[\frac{d}{2}-1\right]}{2^{2d}\pi^d}\frac{L^{-2(1-\varepsilon)}}{1-\varepsilon}$$
$$\times\left\{-\frac{2}{\varepsilon}[\eta(2-\varepsilon,x)-\eta(2-\varepsilon,1-x)]-\frac{8}{\varepsilon}\eta(-\varepsilon)\eta(2-\varepsilon)-\frac{2}{x}+\frac{2}{1-x}\right.$$
$$-4\eta(2)[x\ln(1-x)-(1-x)\ln x]-2\frac{\ln x-1}{x^2}+2\frac{\ln(1-x)-1}{(1-x)^2}-\frac{\pi^2}{\sin^2\pi x}$$
$$\left.-4\eta(2)\ln\tan\frac{\pi}{2}x+4\eta(2)+J^{D,N}(x)+J^{D,N}(1-x)+O(\varepsilon)\right\},\qquad\text{(D61)}$$

where

$$J^{D,N}(x)=4(1-x)J_1^{D,N}(x)-(1-x)J_2^{D,N}(x)+2J_3^{D,N}(x)-J_4^{D,N}(x)\ .\qquad\text{(D62)}$$

In order to evaluate Eqs. (D61) and (D62) we note that

$$J_1^{D,N}(x)=-\eta(2)\ln x-\tfrac{1}{2}[J_3^{D,N}(x)]'\ ,$$
$$J_2^{D,N}(x)=-[J_4^{D,N}(x)]'\qquad\text{(D63)}$$

[see also Eq. (D51)] and use the identity

$$\frac{\pi}{\sin\pi x}=\sum_{n=-\infty}^{\infty}\frac{(-1)^n}{n+x}\qquad\text{(D64)}$$

[see also Eq. (D52)], from which further useful identities follow by taking derivatives with respect to x. We find

$$J_3^{D,N}(x)=-\ln x\left[\frac{\pi}{\sin\pi x}-\frac{1}{x}\right]-\sum_{n\neq 0}(-1)^n\frac{\ln\left[1-\frac{x}{n}\right]}{n+x}\ ,$$
$$\text{(D65)}$$
$$J_4^{D,N}(x)=2\frac{\pi}{\sin\pi x}\ln\frac{\sin\pi x}{\pi}-2\sum_{n\neq 0}(-1)^n\frac{\ln\left[1-\frac{x}{n}\right]}{n+x}$$

and finally obtain, for the two-loop contribution $\bar{e}^{(2)}_{\mathcal{O},SB}(0,z,L)$ to the bare energy density profile for Dirichlet-Neumann boundary conditions,

$$\bar{e}^{(2)}_{\mathcal{O},SB}(0,z,L)=gN\frac{N+2}{12}\frac{\Gamma^2\left[\frac{d}{2}-1\right]}{2^{2d}\pi^d}\frac{L^{-2(1-\varepsilon)}}{1-\varepsilon}\left\{-\frac{2}{\varepsilon}[\eta(2-\varepsilon,x)-\eta(2-\varepsilon,1-x)+2\eta(2-\varepsilon)]-\frac{\pi^2}{\sin^2\pi x}+\frac{\pi^2}{3}\right.$$
$$\left.+2\frac{\pi^2\cos\pi x}{\sin^2\pi x}\left[1+\ln\frac{\pi}{\sin\pi x}\right]-\frac{\pi^2}{3}\ln\frac{\tan(\pi/2)x}{\pi/2}+O(\varepsilon)\right\}.\qquad\text{(D66)}$$

Periodic and antiperiodic boundary conditions are much easier to handle because the one-loop momentum integral in Eq. (D1) does not depend on z' [see Eqs. (C9) and (C10)]. Therefore Eq. (D1) does not involve products of Hurwitz or bivariate η functions in the z' integral, which greatly simplifies the evaluation of $\bar{e}^{(2)}_{\rm per}(0,z,L)$ and $\bar{e}^{(2)}_{\rm aper}(0,z,L)$. We therefore quote only the final results

$$\bar{e}^{(2)}_{\rm per}(0,z,L)=-\bar{e}^{(1)}_{\rm per}(0,z,L)\frac{g}{2^d\pi^{d/2}}\frac{N+2}{3}\frac{\Gamma\left[1-\frac{\varepsilon}{2}\right]}{1-\varepsilon}L^{\varepsilon}2^{1-\varepsilon}\zeta(-\varepsilon)\left[1-\frac{1}{\varepsilon}\right]\qquad\text{(D67)}$$

and

$$\bar{e}^{(2)}_{\rm aper}(0,z,L)=\bar{e}^{(1)}_{\rm aper}(0,z,L)\frac{g}{2^d\pi^{d/2}}\frac{N+2}{3}\frac{\Gamma\left[1-\frac{\varepsilon}{2}\right]}{1-\varepsilon}L^{\varepsilon}2^{1-\varepsilon}\eta(-\varepsilon)\left[1-\frac{1}{\varepsilon}\right].\qquad\text{(D68)}$$

[1] D. J. Amit, *Field Theory, the Renormalization Group, and Critical Phenomena* (McGraw-Hill, New York, 1978).
[2] G. Parisi, *Statistical Field Theory* (Addison-Wesley, Wokingham, 1988).
[3] V. Privman, P. C. Hohenberg, and A. Aharony, in *Phase Transitions and Critical Phenomena,* edited by C. Domb and J. L. Lebowitz (Academic, New York, 1991), Vol. 14, p. 1.
[4] H. W. Diehl, G. Gompper, and W. Speth, Phys. Rev. B **31**, 5841 (1985).
[5] H. W. Diehl, in *Phase Transitions and Critical Phenomena,* edited by C. Domb and J. L. Lebowitz (Academic, London, 1986), Vol. 10, p. 76.
[6] S. Dietrich and H. W. Diehl, Z. Phys. B **43**, 315 (1981).
[7] A. Ciach and H. W. Diehl, Europhys. Lett. **12**, 635 (1990); H. W. Diehl and A. Ciach, Phys. Rev. B **44**, 6642 (1991).
[8] H. W. Diehl and M. Smock, Phys. Rev. B **47**, 5841 (1993).
[9] L. V. Mikheev and M. E. Fisher, Phys. Rev. Lett. **70**, 186 (1993); Phys. Rev. B **49**, 378 (1994).
[10] M. E. Fisher and H. Au-Yang, Physica A **101**, 255 (1980).
[11] J. Rudnick and D. Jasnow, Phys. Rev. Lett. **49**, 1595 (1982).
[12] M. E. Fisher and P. G. de Gennes, C. R. Acad. Sci. Paris Ser. B **287**, 207 (1978).
[13] S. Dietrich and A. Latz, Phys. Rev. B **40**, 9204 (1989).
[14] H. Au-Yang and M. E. Fisher, Phys. Rev. B **21**, 3956 (1980).
[15] J. L. Cardy, in *Phase Transitions and Critical Phenomena,* edited by C. Domb and J. L. Lebowitz (Academic, London, 1987), Vol. 11, p. 55.
[16] T. W. Burkhardt and T. Xue, Phys. Rev. Lett. **66**, 895 (1991); Nucl. Phys. B **354**, 653 (1991).
[17] T. W. Burkhardt and J. L. Cardy, J. Phys. A **20**, L233 (1987); T. W. Burkhardt and H. W. Diehl, Phys. Rev. B **50**, 3894 (1994).
[18] J. L. Cardy, Phys. Rev. Lett. **65**, 1443 (1990).
[19] E. Eisenriegler, M. Krech, and S. Dietrich, Phys. Rev. Lett. **70**, 619 (1993); **70**, 2051 (1993).
[20] E. Eisenriegler, M. Krech, and S. Dietrich (unpublished).
[21] A. A. Belavin, A. M. Polyakov, and A. B. Zamolodchikov, Nucl. Phys. B **241**, 333 (1984); J. Stat. Phys. **34**, 763 (1984).
[22] T. W. Burkhardt and E. Eisenriegler, J. Phys. A **18**, L83 (1985).
[23] T. W. Burkhardt and I. Guim, Phys. Rev. B **36**, 2080 (1987).
[24] T. W. Burkhardt and E. Eisenriegler, Nucl. Phys. B **424**, 487 (1994).
[25] K. Symanzik, Nucl. Phys. B **190**, 1 (1981).
[26] M. Krech and S. Dietrich, Phys. Rev. A **46**, 1886 (1992).
[27] M. Krech and S. Dietrich, Phys. Rev. Lett. **66**, 345 (1991); **67**, 1055 (1991); Phys. Rev. A **46**, 1922 (1992).
[28] V. Dohm, Phys. Scr. **T49**, 46 (1993).
[29] E. Brézin and J. Zinn-Justin, Nucl. Phys. B **257**, 867 (1985); J. Rudnick, H. Guo, and D. Jasnow, J. Stat. Phys. **41**, 353 (1985); E. Eisenriegler and R. Tomaschitz, Phys. Rev. B **35**, 4876 (1987).
[30] W. Huhn and V. Dohm, Phys. Rev. Lett. **61**, 1368 (1988); V. Dohm, Z. Phys. B **75**, 109 (1989).
[31] E. Eisenriegler, Z. Phys. B **61**, 299 (1985).
[32] J. Spanier and K. B. Oldham, *An Atlas of Functions* (Springer, Berlin, 1987).
[33] J C. Le Guillou and J. Zinn-Justin, J. Phys. (Paris) Lett. **46**, L137 (1985).